frontiers | Frontiers in Astronomy and Space Sciences

TYPE Hypothesis and Theory
PUBLISHED 09 February 2026
DOI 10.3389/fspas.2025.1698879

OPEN ACCESS

EDITED BY
Panayiotis Charalambos Stavrinos,
National and Kapodistrian University of Athens, Greece

REVIEWED BY
Elmo Benedetto,
University of Salerno, Italy
Carlos Frajuca,
Federal University of Rio Grande, Brazil

*CORRESPONDENCE
Horst Foidl,
horst.foidl@outlook.com
Tanja Rindler-Daller,
tanja.rindler-daller@univie.ac.at

RECEIVED 04 September 2025
REVISED 21 November 2025
ACCEPTED 28 November 2025
PUBLISHED 09 February 2026

CITATION
Foidl H and Rindler-Daller T (2026) The importance of GR's principle of equivalence for kinematically determined universes and consequences for ΛCDM.
Front. Astron. Space Sci. 12:1698879.
doi: 10.3389/fspas.2025.1698879

The importance of GR's principle of equivalence for kinematically determined universes and consequences for ΛCDM

Horst Foidl[1,2]* and Tanja Rindler-Daller[1,2,3]*

[1]Institut für Astrophysik, Universitätssternwarte Wien, Fakultät für Geowissenschaften, Geographie und Astronomie, Universität Wien, Vienna, Austria, [2]Vienna International School of Earth and Space Sciences, Universität Wien, Vienna, Austria, [3]Wolfgang Pauli Institut, Vienna, Austria

The measurements of the cosmic microwave background (CMB) have determined the cosmological parameters with high accuracy, and the observation of the flatness of space has contributed to the status of the concordance Λ cold dark matter (CDM) model. However, the cosmological constant Λ, necessary to close the model to critical density, remains an open conundrum. The Einstein equations and the Friedmann–Lemaître–Robertson–Walker (FLRW) metric are the foundation of modern cosmology. While the geometric interpretation of the Einstein equations describes the action of gravity as the dynamical curvature of space by matter, the FLRW metric is built on Milne's concept of a kinematically determined Universe. In a preceding companion article, we considered that the Friedmann equation describes the expansion history of FLRW universes in the local reference frame of freely falling comoving observers, who perceive flat, homogeneous, and isotropic space in their local inertial frame. The observed late-time accelerated expansion is then attributed to a kinematic effect akin to a dark energy component. Our approach displayed an expansion history very similar to that of ΛCDM. Now we extend our approach to nonlinear structure formation. We include the impact on the expansion history caused by the cosmic web of the late Universe, once voids dominate its volume, and find that the initially constant w_{de} becomes time-dependent, evolving to a value of $w_{de} \simeq -0.9$ at the present. While this impact of voids is minor, it could provide a possible explanation for the Hubble tension. We use the Cosmic Linear Anisotropy Solving System (CLASS) to calculate the expansion history and power spectra of our extension and compare our results to concordance ΛCDM and to observations. We find that our model agrees well with current data, in particular with the final data release PR4 of the Planck mission.

KEYWORDS

cosmology, kinematic determination, Friedmann–Lemaître–Robetson–Walker metric, spatial curvature, dark energy

1 Introduction

The nature of the cosmological constant Λ has been a challenging open problem in modern cosmology. The issue has intensified over the years, as the current concordance model of ΛCDM, with cold dark matter (CDM) being the other open conundrum, continues to pass many observational tests, especially on the large scales of the cosmic web or the

cosmic microwave background (CMB) radiation. In particular, the CMB measurements have invigorated the flat universe interpretation; that is, that the space of the background universe has no curvature.

However, it was reasoned that the amount of baryonic matter predicted by Big Bang nucleosynthesis was far too small to explain a flat universe (e.g., Steigman, 2007), and even the addition of a substantial amount of dark matter (DM) in the form of CDM, whose presence was not in doubt any longer by the late 1980s, was not sufficient to get a universe at critical density, in order to get a flat geometry of space. In fact, age determinations of the oldest known stars ruled out the Einstein–de Sitter (EdS) model as a viable model, which could have otherwise been a model for a CDM-dominated universe at the present, with its critical density provided by matter only (see, e.g., Weinberg, 2008). Finally, in accordance with the predictions from inflation (Guth, 1981), the observations of the CMB by the balloon-based BOOMERanG experiment (de Bernardis et al., 2000; MacTavish et al., 2006), as well as observations with increasing accuracy by the space missions COBE (Smoot et al., 1992), WMAP (Hinshaw et al., 2013), and Planck (Planck-Collaboration, 2020a), boosted the flat universe interpretation. This, and the previous discovery of the accelerated expansion of the Universe (Perlmutter et al., 1999; Schmidt et al., 1998; Riess et al., 1998; Perlmutter, 2003), led to the empirical addition of the cosmological constant Λ, in order to get a universe at critical density, that is a *flat universe*, and the ΛCDM concordance model became the standard model of cosmology.

Despite the great success of the ΛCDM model, the still unknown nature of CDM and the nature of the cosmological constant Λ, which, according to measurements, each contribute roughly 25% and 70%, respectively, to the present-day energy density of the Universe, remain pending questions. Many cosmological observation campaigns analyze their data, not only in light of testing ΛCDM but also to examine possible extensions to ΛCDM. These extensions replace the cosmological constant Λ with different alternative models of dark energy (DE), which employ a time-dependent equation of state (EOS) parameter $w = p/\rho$. The energy density ρ and the pressure p are commonly understood as components of some physically or operationally defined DE energy-momentum tensor.

Prominent examples of campaigns include the Dark Energy Survey, see, for example, the Year 3 (DES-Y3) results in Abbott et al. (2022) and Abbott et al. (2023) or the CMB measurements by Planck-Collaboration (2020a). They use the so-called "CPL parametrization", given in Equation 1 by Chevallier and Polarski (2001) and Linder (2003) for the EOS parameter,

$$w(a) = w_0 + (1-a)\, w_a, \tag{1}$$

which is defined for $a \in [0,1]$, where a is the scale factor.[1] The CPL parametrization is simple and empirically defined, with no physical motivation for the evolution of $w(a)$ being linear in a.

This article ("Paper III") is a companion to two preceding articles, Foidl and Rindler-Daller (2024) (henceforth Paper I) and Foidl and Rindler-Daller (2025) (henceforth Paper II). We will sometimes, for the sake of brevity and to avoid redundancy, refer the reader to these articles for details. In Foidl and Rindler-Daller (2024), we showed, based on empirical arguments, that a cosmological model including a CPL-based DE component with an EOS parameter w_{de} evolving from -0.8 to -0.9 describes the CMB temperature spectrum of ΛCDM and yields a Hubble constant H_0 that is compatible with direct measurements (e.g., Riess et al., 2022) in the local Universe. In Foidl and Rindler-Daller (2025), we showed that the phenomenology of a late-time accelerated expansion is explained in a very natural way as a kinematic effect, once the concept of a kinematically determined universe and general relativity (GR)'s principle of equivalence are considered stringently. We incorporated the kinematic effect into the Friedmann–Lemaître–Robertson–Walker (FLRW) formalism as a kinematical DE component, with a constant EOS parameter w_{de}. Its value depends on the number of physical components of the Universe, where the kinematic DE component is not considered a physical component. In this Paper III, we present proposals as extensions to ΛCDM—wCDM and owCDM—with a time-dependent EOS parameter w_{de} of its kinematic DE component evolving from -0.8 to -0.9, which we would like to put up for discussion. We use these acronyms for our models, as they are used frequently in the literature to express an extension to ΛCDM, particularly for dynamical dark energy (DDE) models, without and with spatial curvature, respectively (see, e.g., Dark Energy Survey Year 3 Results (Abbott et al., 2023), Planck-Collaboration (2020a), and the Particle Data Group Review, Chapter 28 "Dark Energy" (Group et al., 2022)).

We include in our ΛCDM extension the effects of the cosmic voids, which dominate the volume of the Universe in the late stages of the evolution of the cosmic web. The resulting backreaction from voids also affects the evolution of the expansion rate. We consistently include this effect into $\rho_{\rm de}$, using void models informed by cosmological ΛCDM simulations of the previous literature, and parameterize it by deriving the necessary modifications to the heretofore constant EOS parameter $w_{\rm de}$, which becomes a function of time, or scale factor, respectively, once the voids dominate the volume of the Universe. In fact, the initial value of $w_{\rm de}(a) \sim -0.8$ decreases to $w_{\rm de}(1) \sim -0.9$ at the present where the scale factor $a = 1$. Thus, it gets closer to the EOS of a cosmological constant. As a result, the present-day value of the expansion rate H_0, that is, the Hubble constant, shifts to a higher value, compared to the value it would have if the EOS parameter remained constant throughout cosmic time (see also Foidl and Rindler-Daller, 2024). Although the expansion rate is changed by only approximately 8% due to the impact of voids, it is enough to provide a possible solution to the Hubble tension problem.

By comparing our results with cosmological observations, we find that our ΛCDM extension agrees with current data. To this end, we apply our proposed procedure by Foidl and Rindler-Daller (2024) to our model and fit it to the ΛCDM CMB spectrum and $H_0 = 73.04$ km/s/Mpc as determined by Riess et al. (2022) in the local Universe, where we, in addition to wCDM, consider also spatial curvature. The resulting owCDM model perfectly agrees with the final results of the Planck mission (Tristram et al., 2024), in particular with the reported spatial curvature of $\Omega_{k,0} = -0.012 \pm 0.010$.

This article is organized as follows. In Section 2, we recapitulate the basic equations for the evolution of the background universe in FLRW models. Section 3 contains our treatment and derivation of

1 In practice, cosmological codes in the default configuration, including the one we use (CLASS), compute observables not earlier than at $a = 10^{-14}$.

the impact of cosmic voids on the expansion history. This impact is minor but significant enough to provide a possible resolution to the Hubble tension problem. In the following Section 4, we present the results of the numerical simulations of our ΛCDM extension wCDM, based on our amended version of the Cosmic Linear Anisotropy Solving System (CLASS) code, where we also compare our results with the concordance ΛCDM model, as well as with observations. In Section 5, we present the results of our owCDM model and compare it to Planck's PR4 (Tristram et al., 2024). Finally, in Section 6, we summarize the presented concepts, results, and implications in light of cosmological observations.

2 Basic equations for the expansion history in FLRW models

First, we briefly recapitulate the well-known equations describing the evolution of the homogeneous and isotropic background universe, which we need in the following. For a detailed introduction to the equations, we refer the reader to Foidl and Rindler-Daller (2025).

As gravity is the only force acting on cosmological length scales, it determines the evolution of the background universe and is described by Einstein's field equations:

$$R_{\mu\nu} - \frac{1}{2} g_{\mu\nu} \mathcal{R} = \frac{8\pi G}{c^4} T_{\mu\nu}, \tag{2}$$

with the Ricci tensor $R_{\mu\nu}$ and the Ricci scalar $\mathcal{R}$. The left-hand side (lhs) of the equation is often expressed as $E_{\mu\nu}$, the Einstein tensor. The right-hand side (rhs) contains the energy–momentum tensor $T_{\mu\nu}$, which includes the cosmic inventory of given cosmological models. Cosmological models differ in their assumptions on the nature and amount of the cosmic components encoded in $T_{\mu\nu}$.

Robertson (1935), Robertson (1936a), Robertson (1936b), and Walker (1937) developed a metric describing the geometry of a universe with constant curvature based on Milne's idea of a kinematically determined universe. In spherical coordinates (r, θ, ϕ), the line element of the metric reads as:

$$ds^2 = c^2 dt^2 - a^2(t) \left(\frac{dr^2}{1 - kr^2} + r^2 d\Omega^2 \right), \tag{3a}$$

$$d\Omega^2 = d\theta^2 + \sin^2 \theta d\phi^2, \tag{3b}$$

where k is the curvature index, its values are +1 (closed universe), 0 (flat universe), and −1 (open universe), and a is the scale factor.

Applying the FLRW metric (Equations 3a, 3b) to the metric tensor $g_{\mu\nu}$ in the Einstein Equation 2, the time–time component yields the (first) Friedmann equation in the *classical version*, as derived by Friedmann (1922):

$$H^2(t) = \frac{8\pi G}{3c^2} \rho - \frac{kc^2}{a^2(t)}, \tag{4}$$

which describes the dynamics of the evolution of the background universe in the reference frame of a free-falling observer, comoving with the expansion,[2] moving on a geodesic (in a possibly curved space). H is the Hubble parameter (we use the term "expansion rate" interchangeably), defined as Equation 5:

$$H(t) = \frac{\dot{a}}{a}, \tag{5}$$

where the dot refers to the derivative with respect to cosmic time t.

The Friedmann equation in *modern* language reads as:

$$H^2(t) = \frac{8\pi G}{3c^2} \left[\rho_r(t) + \rho_b(t) + \rho_{\mathrm{CDM}}(t) + \rho_k(t) + \rho_\Lambda(t) \right], \tag{6}$$

with the time-dependent background energy densities for radiation (ρ_r), baryons (ρ_b), CDM (ρ_{CDM}), the curvature (ρ_k), and the cosmological constant (ρ_Λ). $H(t)$ is the Hubble parameter, and its present-day value,[3] the Hubble constant, is denoted as H_0. The critical density, defining a flat universe (i.e., a universe with flat geometry), is given by:

$$\rho_{\mathrm{crit},t} = \frac{3H^2(t) c^2}{8\pi G}, \tag{7}$$

derived from Equation 4 with vanishing curvature term. It is convenient to introduce the so-called density parameters or cosmological parameters defined in Equation 8:

$$\Omega_{t,i} = \frac{\rho_i(t)}{\rho_{\mathrm{crit},t}}, \tag{8}$$

where $i =$ CDM, b, r, etc., and which are nothing but the background energy densities relative to the critical density expressed by Equation 7.

To solve the Friedmann equation, customarily, the energy conservation equation is applied (for each component i = CDM, b, r, …), which reads:

$$\frac{\partial \rho_i}{\partial t} + 3H(\rho_i + p_i) = 0, \tag{9}$$

where ρ_i and p_i stand for the respective background energy densities and pressures.[4] The energy densities and pressures are each related by their respective EOS:

$$p_i(t) = w_i(t) \rho_i(t), \tag{10}$$

where w_i is often called the EOS parameter, which can also change with time, in general. However, in ΛCDM, w_i is assumed to be a constant[5] for every component i = CDM, b, r, Λ, and k. Assuming a constant EOS parameter w_i and using Equation 10 in Equation 9 yields the well-known relationship:

$$\rho_i(a) = \Omega_{i,0} \rho_{\mathrm{crit},0}\, a^{-3(1+w_i)}, \tag{11}$$

2 The comoving observer is called the fundamental observer by Robertson (1935). This term is also sometimes used in the literature.

3 The literature has adopted the notational subscript "0" to denote present-day values, not the values at $t = 0$.

4 This equation assumes that there is no transformation between different components.

5 However, for a detailed study of phase transitions in the early Universe, it is important to include, for example, a variable EOS of the radiation component, to consider the reduction of relativistic degrees of freedom in the wake of the Universe's expansion.

which describes the evolution of the background energy densities as a function of the scale factor a for constant w_i. The background evolution of the standard cosmic components is given by:

$$\rho_r(a) = \Omega_{r,0}\rho_{\mathrm{crit},0}/a^4, \tag{12a}$$
$$\rho_m(a) = \Omega_{m,0}\rho_{\mathrm{crit},0}/a^3, \tag{12b}$$
$$\rho_k(a) = \Omega_{k,0}\rho_{\mathrm{crit},0}/a^2, \tag{12c}$$
$$\rho_\Lambda = \Omega_{\Lambda,0}\rho_{\mathrm{crit},0}. \tag{12d}$$

We have Equation 12a for radiation (its EOS parameter in Equation 10 is $w_r = 1/3$), Equation 12b for baryonic matter and for CDM ($w_m = 0$), Equation 12c for curvature ($w_k = -1/3$), and Equation 12d for the cosmological constant Λ ($w_\Lambda = -1$).

The Friedmann equation for the ΛCDM model, (Equation 6), can be alternatively written as an algebraic closure condition. At the present, it reads:

$$1 = \Omega_{r,0} + \Omega_{b,0} + \Omega_{\mathrm{CDM},0} + \Omega_{k,0} + \Omega_{\Lambda,0}. \tag{13}$$

In other words, Equation 13 is the normalization of the Friedmann Equation 6 to the critical density. In the ΛCDM model, $\Omega_{k,0} = 0$ is prescribed, such that Λ closes the Universe to critical density, defining it as a flat Universe, which we have elaborated on in Foidl and Rindler-Daller (2025).

Our approach presented in Foidl and Rindler-Daller (2025) replaced Λ with a "kinematic DE component" and a constant EOS parameter w_{de}, which reads as:

$$w_{\mathrm{de}} = \frac{2}{3}\Omega_{\mathrm{phys},0} - 1, \tag{14}$$

where $\Omega_{\mathrm{phys},0}$ denotes the total of the density parameters for the physical contributions to the energy content of the Universe (matter and radiation) at the present. Therefore, w_{de} is constant.

To retain ΛCDM's formalism and Equation 11 (see also Foidl and Rindler-Daller (2025)), we make a distinction of cases. We apply the constant value of $w_{\mathrm{de}} = -1/3$ to flat and closed geometries, as is also the case in ΛCDM (with $w_k = -1/3$). For open geometries, we apply Equation 14. In summary, we have:

$$w_{\mathrm{de,early}} = -\frac{1}{3} - \Theta(\Omega_{\mathrm{de},0})\frac{2}{3}\Omega_{\mathrm{de},0}, \tag{15a}$$
$$\Omega_{\mathrm{de},0} = 1 - \Omega_{\mathrm{phys},0}. \tag{15b}$$

In Equation 15a Θ is the Heaviside function and Equation 15b defines DE's density parameter. We use the additional subscript "early" to express that this is the initial value for the EOS parameter in the early Universe. In Section 3, we will show that in the regime of nonlinear structure formation, the EOS will morph from a constant value to a time-dependent (or scale-factor-dependent) function.

The Heaviside function separates the two regimes of super- and subcritical model universes. The first term corresponds to deceleration due to the critical density. The factor after the Heaviside function applies to subcritical universes only, where $w_{\mathrm{de,early}}$ falls below $-1/3$; that is, a decreasing EOS parameter implies less deceleration, as it should. In addition, we retain $\Omega_{k,0} = 0$ to express the perceived flatness of space, in our local inertial frame as comoving FLRW observers, in the same way as in ΛCDM. There is a degeneracy for the impact of spatial curvature on the CMB spectrum with the cosmological constant Λ or dark energy, respectively; see, for example, Hu and Dodelson (2002). We will get back to this point in Section 5.

Finally, the Friedmann Equation 16a reads:

$$H^2(t) = \frac{8\pi G}{3c^2}\left[\rho_r(t) + \rho_b(t) + \rho_{\mathrm{CDM}}(t) + \rho_{\mathrm{de}}(t)\right], \tag{16a}$$
$$\rho_{\mathrm{de}}(a) = \Omega_{\mathrm{de},0}\rho_{\mathrm{crit},0}\, a^{-3(1+w_{\mathrm{de,early}})}. \tag{16b}$$

Equation 16b now describes the evolution of ρ_{de} as a function of scale factor a for a constant $w_{\mathrm{de,early}}$, given by Equations 15a, 15b. The present-day critical density $\rho_{\mathrm{crit},0}$ is defined in Equation 7. For more detail, see Foidl and Rindler-Daller (2025).

3 The expansion history in the nonlinear regime

In Foidl and Rindler-Daller (2025), we presented an extension to ΛCDM, which abandons the cosmological constant Λ in favor of an approach that describes the DE phenomenology as a kinematic effect, induced by the primeval expansion rate H_{ini} post Big Bang in relation to the initial density, to extend the ΛCDM model beyond the fine-tuned case of a Universe at critical density.

In ΛCDM, the nonlinear stage of structure formation is assumed to have no impact on the evolution of the background universe. In this section, we reassess the possibility of such an impact. More precisely, we investigate the impact of the formation of the cosmic web, in particular of its voids, on the expansion history. We can show that there is an impact, which is minor but significant enough to explain the Hubble tension problem, on which we elaborate in detail below.

To motivate our approach, we reconsider first the ideas around the issue of a backreaction from structure formation, particularly in the late stages of the evolution of the cosmic web, because by then, voids dominate the volume of the Universe.

3.1 The evolution of the voids

The pioneering work of Icke (1984) showed that voids evolve into spherical shapes and become distributed homogeneously during the formation of the cosmic web. The following works by Icke and van de Weygaert (1987), van de Weygaert and Icke (1989), and van de Weygaert (1994) presented analytical descriptions of the evolution of the cosmic web, based on the Voronoi tessellation (Voronoi, 1908, see also Okabe et al., 2000). Icke and van de Weygaert (1991) confirmed the correctness of this approach by comparing it to observations. Analytical approximations presented in Icke (2001) describe the evolution of the individual components of the cosmic web as Voronoi features, which we display here as Equations 17a–d:

$$m_v = e^{-3\theta}, \tag{17a}$$
$$m_w = 3e^{-2\theta}\left(1 - e^{-\theta}\right), \tag{17b}$$
$$m_f = 3e^{-\theta}\left(1 - e^{-\theta}\right)^2, \tag{17c}$$
$$m_n = \left(1 - e^{-\theta}\right)^3, \tag{17d}$$

where θ is a measure of time,[6] with $\theta \propto t^{2/3}$ in a matter-dominated universe. The quantities m_x denote the mass fractions of the individual components of the cosmic web: (a) m_v for the voids, (b) m_w for the walls, (c) m_f for the filaments, and (d) m_n for the nodes.

As voids became a subject of interest, Colberg et al. (2005) and Shandarin et al. (2006) derived density profiles, shapes, and sizes from cosmological simulations. Ricciardelli et al. (2013) showed that voids display a universal density profile. Cautun et al. (2014) derived the evolution history of the individual components of the cosmic web from the Millennium simulation of Springel et al. (2005).

3.2 The backreaction problem

The expansion history of the Universe in the ΛCDM model is determined by the solution of the Friedmann equations, applying the average energy density of the background universe. This is a valid approach, as long as the distribution of the energy densities can be considered homogeneous and isotropic, that is, in the early Universe. However, the cosmological principle is no longer valid in the late Universe on spatial scales of the order of approximately Gpc and below. Thus, averaging the density of the Universe and solving the Friedmann equations by neglecting this nonlinear structure formation is problematic. This is known in cosmology as the *averaging problem*. The theoretical background of this problem arises from the nonlinearity of the Einstein Equation 18:

$$E_{\mu\nu} = \frac{8\pi G}{c^4} T_{\mu\nu}, \tag{18}$$

first pointed out by Ellis (1983). Averaging the metric in an inhomogeneous environment first, before solving the Einstein equations, will lead to an additional correction term $C_{\mu\nu}$ in the averaged Einstein Equation 19:

$$\langle E_{\mu\nu} \rangle = \frac{8\pi G}{c^4} \langle T_{\mu\nu} \rangle + C_{\mu\nu}. \tag{19}$$

The questions to be addressed are the following: (a) can this term reach relevant orders of magnitude to influence the expansion history of the Universe? (b) Does perturbation theory eventually break down?

In ΛCDM, it is assumed that the correction term $C_{\mu\nu}$ is negligible. On the other hand, if this term were found to impact the expansion history, it would be seen as a *backreaction process*, caused by inhomogeneities in the background universe.

Questions (a) and (b) have been explored in the literature, providing basically the following answers: in case the size of perturbations is much smaller than the (time-dependent) Hubble sphere, the correction term does not have a substantial impact on the expansion history and can be neglected. This means it cannot explain the phenomenology of the accelerated expansion (see, for example, Kolb et al., 2005; Notari, 2006; Li and Schwarz, 2007; Räsänen, 2006a; Buchert, 2000; Buchert, 2001; Kwan et al., 2009; Paranjape, 2009).

Paranjape (2009) explored the averaging problem and its importance in cosmology in a mathematically rigorous way. They constructed a toy universe based on the Lemaître–Tolman–Bondi (LTB) metric (Lemaître, 1933; Lemaître and MacCallum, 1997; Tolman, 1934; Bondi, 1947). The key property of this metric is that it allows radial inhomogeneities while preserving isotropy. Their model was centered at an over-dense spherical region, a model for a formed dark matter halo, surrounded by an under-dense shell. The remaining part of the universe was regarded as homogeneous out to the Hubble sphere. They found that the value of the correction term $C_{\mu\nu}$ induced by the inhomogeneity is too small to have an impact on the expansion history, justifying the assumptions of ΛCDM. However, while the toy model analyzed in Paranjape (2009) perfectly fits the regime of halo formation and virialization, it does not apply to the late stages of cosmic web formation, once voids dominate the volume of the Universe.

Buchert (2011) also investigated the averaging problem, based on the LTB metric, and found that the global backreaction in a flat LTB model vanishes in a spherical domain. This result is compatible with the interpretation of the Universe to appear homogeneous, if we choose a large enough spatial scale, that is, $\gtrsim 100$ Mpc at the present (Hogg et al., 2005; Scrimgeour et al., 2012), justifying the assumptions in ΛCDM. Moreover, Buchert and Ehlers (1997) have shown that in 3D-torus architecture, global backreaction vanishes, as well, meaning that in cosmological simulations with periodic boundary conditions, backreactions cannot appear.

3.3 The backreaction from voids

Although backreaction from the averaging problem has been shown to vanish in LTB models, Buchert et al. (2015) demonstrated that there is no proof that backreaction by inhomogeneities is, in general, negligible in cosmology. Amendola and Tsujikawa (2010) and Kolb et al. (2005) pointed out that the result of the averaging problem is very sensitive to the way the average is performed.

In this article, we reconsider the averaging problem as applied to the late stages, when voids dominate the volume of the Universe. More precisely, we distinguish the impact of density vs. volume. In the late stages of nonlinear structure formation, the Universe is dominated in volume by a homogeneous distribution of spherical voids of very low density, embedded in a highly over-dense region, which occupies only a minor fraction of the volume of the Universe. This picture is compatible with the general-relativistic "separate universe conjecture" (Weinberg, 2008), which states that a spherically symmetric region in a homogeneous and isotropic universe behaves like a mini universe. There are three approaches, which can each support the conjecture that voids as the dominating volume fraction of the Universe influence the expansion history: a) a phenomenological approach, b) a backreaction process, and c) results of simulations, supported by d) results from observations, as discussed next.

3.3.1 Phenomenological approach

Following the separate universe conjecture, every void can be considered a mini universe with its own expansion rate. Moreover, we do not consider the evolution of a single void, but in a holistic view, we consider the entire Hubble sphere.

6 Not to be confused with θ in the FLRW metric (Equations 3a, 3b).

The expansion rate of the Universe decreases with time, due to the action of gravity. This deceleration is determined by the gravitational forces F_G between any two points (p_1,p_2) in the homogeneous universe. Following Birkhoff's theorem (Birkhoff and Langer, 1923; Jebsen, 1921; Maciel et al., 2018), gravitational forces in a homogeneous sphere are proportional to the distance r between any point p from the center p_c: $F_G \propto r(p,p_c)$. Considering points p_x at the edge of an over-dense region surrounding a very under-dense void yields the usual Newtonian law of gravity $F_G \propto 1/r^2(p_x,p_c)$. This can be applied to the scenario where voids are embedded in an over-dense environment, showing that deceleration in the voids is less pronounced than in the surrounding cosmic web. Alternatively, this can also be seen by Birkhoff's theorem for the spherical low-density voids, yielding a lower gravitational force within the voids than their higher-density homogeneous environment. This means that voids are experiencing an accelerated expansion, compared to their higher-density homogeneous environment. As long as voids do not dominate the volume of the Universe, this expansion can be compensated by the "congestion" of the over-dense walls and filaments. As soon as voids begin to dominate the volume of the Universe, this compensation fails. Voids dominate the volume of the Universe and therefore the expansion of the Universe, as it is directly connected to the volume of the voids.

3.3.2 Backreaction process

The solutions to the averaging problem, which we present in Section 3.2, consider the size of inhomogeneities clearly smaller than the Hubble radius. Therefore, it is always possible to find a minimum spatial scale above which the Universe can be considered homogeneous, yielding no impact on the expansion history.

However, as studies have shown, in the case that the perturbations are of the size of the Hubble radius or even larger ("superhorizon modes"), the correction term can grow to significant values and therefore may impact the expansion history of the Universe, which appears as a classical (zero-momentum) background (see, e.g., Carloni et al., 2008; Martineau and Brandenberger, 2005; Barausse et al., 2005; Kolb et al., 2005; Parry, 2006; Kumar and Flanagan, 2008; Hirata and Seljak, 2005; Flanagan, 2005; Räsänen, 2006b; Geshnizjani et al., 2005). This topic is subject to controversial discussions, and whether such huge perturbations exist at all has been questioned (see, e.g., Carloni et al., 2008; Stoeger et al., 2007; Wetterich, 2003; Calzetta et al., 2001; Siegel and Fry, 2005; Gasperini et al., 2009; Gruzinov et al., 2006; Notari, 2006; Van Acoleyen, 2008).

Yet, relativistic perturbation theory does predict superhorizon perturbations, and as the Hubble sphere grows over time, more and more such perturbations enter that sphere (perturbations leave the sphere, once the scale factor grows exponentially and $H = const$). Either way, it appears that these superhorizon perturbations are far too sub-dominant to source a backreaction process onto the background evolution to explain the phenomenology of the accelerated expansion.

In our model, we take into account the evolutionary stage of the cosmic web, once voids dominate the volume of the Universe: low-density spherically symmetric voids are embedded in a highly over-dense homogeneous background. We consider the impact of the entire cosmic web on the backreaction process, encompassing the entire Hubble sphere. Therefore, we can regard the entirety of all voids as *one* huge, extremely low-density region, appearing as a classical (zero-momentum) background; see, for example, Barausse et al. (2005) and Kolb et al. (2005). The solutions to the averaging problem presented in Section 3.2 are based on the isotropy of the Universe, as they apply the LTB metric that allows radial inhomogeneities, while preserving isotropy. Our approach, however, allows for small anisotropies in the cosmic web because we consider its structure, ever since voids dominate the volume of the Universe and the cosmological principle no longer holds true on spatial scales of approximately Gpc and below. This induces a small backreaction onto the background universe (see Subsection 3.4) and offsets us from an ideally comoving observer (see Section 5).

3.3.3 Backreaction via spatial averaging

Let us add another aspect of the backreaction. Buchert et al. (2015) showed that, in general, there is no proof that inhomogeneities are negligible in background cosmology. Nevertheless, the success of the ΛCDM model suggests that any impact of inhomogeneities on the expansion rate should be weak. However, Wiltshire (2007) and Wiltshire (2011) showed that, particularly, in the late stages of the evolution of the cosmic web, averaging and coarse-graining are problematic procedures.

Rácz et al. (2017) performed a cosmological N-body simulation, integrating the Newtonian equations, as is customary in cosmological simulations (e.g., Springel et al., 2005), with a changing general-relativistic metric, which is calculated from spatially averaged quantities. The result indicated that for a typical spatial scale of the averaging procedure, an impact on the expansion history with deviations from the results based on the FLRW metric is possible.

Before we close this subsection, we reiterate that all studies indicate that the backreaction onto the background evolution, including the backreaction from voids, cannot "explain away" the phenomenology of accelerated expansion. However, by including the minor backreaction of voids that we find, we can possibly resolve the Hubble tension problem, as shown below. Recent studies, for example, by Koksbang (2021) and Koksbang (2022), explored the feasibility of the detection of signals of a backreaction in cosmological measurements and reported constraints for the backreaction process and its impact on H_0, compatible with the results of our model which we present in the next section.

3.3.4 Results from observations

As discussed in a later section, recent work by, for example, Dainotti et al. (2022b), Dainotti et al. (2021), Dainotti et al. (2022a), Bargiacchi et al. (2023b), Bargiacchi et al. (2023a), Ó Colgáin et al. (2021), and Krishnan et al. (2021), indicates that the evolution of the expansion rate H at low redshift conflicts with the assumption of a cosmological constant. These results may indicate that the origin of the Hubble tension is likely to be in cosmology and not in local measurement issues, where a dynamical DE component, our proposed model, or a backreaction from the late stages of structure formation might each *a priori* constitute a solution.

3.4 Including backreaction into the ΛCDM extension

There is a straightforward approach to incorporate the backreaction from the cosmic web and its voids into the ΛCDM extension, and at the same time to quantify the corresponding impact on the expansion history, as follows. We apply the hydrodynamical and geometrical models from Icke (1984), Icke and van de Weygaert (1987), and Icke (2001) for the formation of the cosmic web and extract the relevant quantities from the analysis by Cautun et al. (2014) of the Millennium simulation. The advantage of this procedure is the fact that the large-scale structure of the Universe in our model is informed by cosmological ΛCDM simulations, which are in good agreement with observations, that is, with large galaxy surveys on scales of the cosmic web.

In the ΛCDM extension, which we presented in Foidl and Rindler-Daller (2025), the cosmological constant Λ is replaced by an "operational dark energy," where the associated EOS is given in Equations 15a, 15b. As previously mentioned, the expansion of the voids is directly connected to the expansion of the Universe by their dominance in volume and their low density. Therefore, it is straightforward to express the impact of voids on the expansion history through the EOS of $\rho_{\rm de}$. As a result, the initially constant EOS parameter $w_{\rm de,early}$ morphs into a time-dependent function. This makes sense because voids become important only at the later stages of structure formation. To quantify this effect, we use the results derived by Cautun et al. (2014), who analyze the evolution of the cosmic web and derive the evolution of the mass fractions and volume fractions for the individual components of the cosmic web (i.e., voids, filaments, walls, and nodes), using the Millennium simulation by Springel et al. (2005). Cautun et al. (2014) find that voids dominate the volume of the Universe as of a redshift $z \sim 5$. The analytical model given in Equations 17a–d from Icke (2001) shows that the matter fraction of the voids evolves linearly in redshift, to a good approximation, in the late stages of the evolution of the cosmic web.

We apply both findings to our Equation 15a to derive the following linear approximation for the evolution of the EOS parameter of $\rho_{\rm de}$ as a function of the scale factor as follows. We use Equation 15a to obtain the $w_{\rm de,early}$ (from parameters reported by Planck-Collaboration (2020a)) and $w_{\rm de,0}$ (from the results reported by Cautun et al. (2014)). In the linear evolution of redshift from $z = 5$ to $z = 0$, we use $z + 1 = 1/a$ to express $w_{\rm de}$ as a function of scale factor a, which yields:

$$w_{\rm de}(a) = \begin{cases} w_{\rm de,early} & \text{when } a \le 1/6 \\ w_{\rm de,early} + \left[\dfrac{(1/a-1)-5}{5}\right]\left(w_{\rm de,early} + 0.9\right), & \\ \text{when } a \le 1/6. & \end{cases} \tag{20}$$

Thus, the EOS parameter $w_{\rm de}$ becomes a function of cosmic time, or scale factor, respectively, as indicated in the formula, once the scale factor has reached the threshold determined by the aforementioned analysis. Using density parameters for our model of $\Omega_{\rm de,0} = 0.7$ and $\Omega_{m,0} = 0.3$, we get $w_{\rm de}(1) \sim -0.9$ for the present-day EOS parameter. Comparing this result with the constant EOS parameter $w_{\rm de,early} = -0.8$ of Foidl and Rindler-Daller (2025), we see that the impact of voids leads to a more negative EOS parameter, with a value closer to that of a cosmological constant. In fact, this is an expected outcome, given the dynamics of voids. The recent study by Dinda (2023) also reports that a non-phantom behavior of DE proves more favorable in both wCDM and CPL models across diverse data combinations. In contrast, the recent Dark Energy Spectroscopic Instrument (DESI) data release reports a phantom-energy-type DE component as an alternative to Λ, which we discuss in Section 6.

To reflect the correct evolution of the background, we stress that the time-dependence of the EOS parameter requires a forward-in-time integration of the energy conservation Equation 9 to determine the evolution of the energy density $\rho_{\rm de}$. Thus, Equations 11, 16b, respectively, cannot be used naively. Regarding this important point, we refer the reader to Foidl and Rindler-Daller (2024), where we discussed in detail computational characteristics for cosmological models with a dynamical dark energy component and the implications of a decreasing vs. increasing EOS parameter.

We mentioned already that the impact of voids makes the EOS parameter $w_{\rm de}$ more negative than without this impact. In fact, as the density within voids decreases while their volume increases, $w_{\rm de}(a)$ will converge asymptotically to the EOS parameter $w_{\rm de} = -1$ of a cosmological constant.

4 Results for the wCDM extension to ΛCDM

In order to accurately calculate the background evolution of our ΛCDM extension and to compare it carefully with the concordance ΛCDM model and with observations, we use the open-source cosmological Boltzmann code CLASS,[7] which is designed not only to provide a user-friendly way to perform cosmological computations but also to provide a flexible coding environment for implementing customized cosmological models. The modular architecture allows enhancing the code without compromising existing functionality. The underlying concepts, including an overview of coding conventions, are presented in Lesgourgues (2011). This version uses the Planck 2018 cosmological parameters from Planck-Collaboration (2020a) as the default parameter set. Additionally, the configuration provides different sets of precision configuration files to reflect varying requirements on precision, which may be needed in the results or available computation time. The precision configuration with the highest accuracy has been proved to be in conformance with the Planck results within a level of 0.01%. Therefore, it is sufficient to compare the results of the simulation for our model to the results of the simulations for ΛCDM to ensure agreement with the results of the CMB measurements.[8]

We use the fiducial parameters of the ΛCDM model from Planck-Collaboration (2020a), shown in Table 1, in our calculations. We properly implemented the equations of our ΛCDM extension Equations 15, 16 and Equation 20 into the background module of CLASS, as well as into the perturbation module, because we also calculated and compared the CMB temperature spectra between

7 The code CLASS is publicly available at http://class-code.net/.

8 Planck PR4 (Tristram et al., 2024) also uses CLASS in its Bayesian analysis of the CMB measurements.

TABLE 1 Cosmological parameters used in the computations.

Parameter	Value	Comment
H_o	67.556	
T_{CMB} [K]	2.7255	
N_{ur}	3.046	
$\Omega_{r,0}$	5.41867×10^{-5}	Derived from T_{CMB}
$\Omega_{\nu,0}$	3.74847×10^{-5}	Derived from N_{ur}
$\Omega_{b,0}$	0.0482754	
$\Omega_{CDM,0}$	0.263771	
$\Omega_{de,0}$, $\Omega_{\Lambda,0}$	0.687762	wCDM, ΛCDM
$\Omega_{k,0}$	0	
τ_{reio}	0.0925	
A_s	2.3×10^{-9}	
n_s	0.9619	Adiabatic ICs

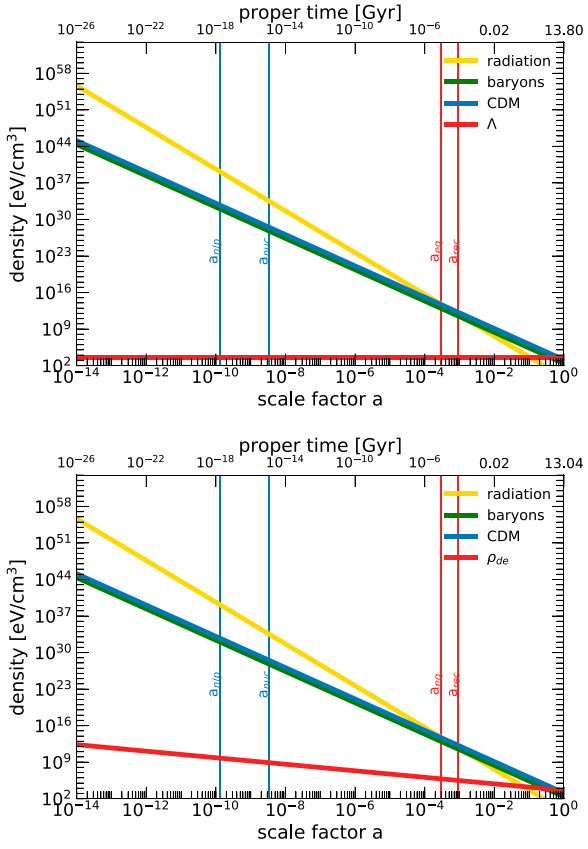

FIGURE 1
Evolution of energy densities in ΛCDM (top panel) and wCDM (bottom panel) as a function of scale factor and proper time, respectively. The top panel displays the evolution of the individual contributions to the energy density of the ΛCDM model according to Equations 12a–d. The solid red line indicates the evolution of the cosmological constant Λ. The bottom panel displays the evolution of the individual contributions to the energy densities of the wCDM model. The radiation and matter components show no differences compared to ΛCDM. However, the solid red line for ρ_{de} is not a constant but has a slope, corresponding to $w_{de,early} \sim -0.8$, according to Equations 15a, 15b. Note that the late impact of voids on $w_{de,early}$ is not recognizable in the log–log plot. The vertical lines in blue bracket the epoch of Big Bang nucleosynthesis, between neutron–proton freeze-out at $a_{n/p} \sim 1.3 \cdot 10^{-10}$ and nuclei production $a_{nuc} \sim 3.3 \cdot 10^{-9}$, while the vertical lines in red (at larger scale factor) indicate the time of matter–radiation equality a_{eq}, followed by recombination a_{rec} (see also Figure 2).

our ΛCDM extension and concordance ΛCDM, as presented in the next section.

Two CLASS simulations were run to compare the results of our ΛCDM extension to the concordance ΛCDM model. The first run was performed using the unmodified version of CLASS. The second run used our amended version of CLASS with parameters according to Table 1. In what follows, we designate the cosmological constant by Λ, as is customary. The effect of DE in the ΛCDM extension is denoted by ρ_{de}, w_{de}, and Ω_{de}, respectively. ΛCDM refers to the concordance model, whereas the ΛCDM extension is denoted as "wCDM." This notion is often associated with the specific CPL parametrization, by Chevallier and Polarski (2001) and Linder (2003) for the EOS parameter, whereas we use it to refer to our own parametrization in Equation 20.

4.1 Evolution of densities and equation of state

Figure 1 displays the evolution of the energy densities ρ_i vs. scale factor a, as well as vs. proper time, in both models.

The top panel displays the evolution of the densities in the ΛCDM model, corresponding to the individual components of the Universe, as indicated in the legend. The slopes of the individual curves are as expected from Equations 12a–d. The solid red line depicts Λ, showing a constant evolution as expected for the cosmological constant. The bottom panel displays the evolution of the energy densities in the wCDM model. In this model, the early slope of the red curve for ρ_{de} corresponds to the EOS parameter $w_{de,early} \simeq -0.8$, determined by Equation 15 and Equation 20. The vertical lines in blue bracket the epoch of Big Bang nucleosynthesis, between neutron–proton freeze-out at $a_{n/p} \sim 1.3 \times 10^{-10}$ and nuclei production at $a_{nuc} \sim 3.3 \times 10^{-9}$, while the vertical lines in red (at larger scale factors) indicate the time of matter–radiation equality $a_{eq} \sim 10^{-4}$, followed by recombination $a_{rec} \sim 10^{-3}$ (the detailed numbers for the latter depend somewhat more upon the cosmological model). The effect of the backreaction from voids in the late stages of the evolution is so small that it cannot be recognized in the log–log plot. The evolution of the matter and radiation components indicates no significant differences between the two models, as expected.

However, the ages of the models differ, as can be seen from the value of the proper time at the very present. The ΛCDM model has an age of 13.8 Gyr, whereas the age of the wCDM model is 13.04 Gyr. In Section 4.3, where we discuss the Hubble tension

problem, we will present arguments to show that the lower age of the wCDM universe is no obstacle to the model.

Figure 2 displays the evolution of the density parameters Ω_i (as indicated in the legends) vs. scale factor a and proper time, respectively, for both models. The panels display both the $\Omega_{\rm de}$ of wCDM (solid red curve) and the Ω_Λ of ΛCDM (dotted red curve). We can see that the $\Omega_{\rm de}$ of wCDM gets to be the dominant contribution to the energy budget of the Universe at a smaller scale factor than the Ω_Λ of ΛCDM. As an illustration, we include the green-hatched vertical band, which indicates the range of redshifts (resp. scale factors) of the sample of galaxies used by the Supernova Cosmology Project (Perlmutter et al., 1999). It was one of the high-redshift SNe Ia surveys that discovered the accelerated expansion in the late 1990s. The bottom panel displays the same quantities but shows a zoom-in to highlight the range of scale factors from $a = 0.1$ to 1. While the advanced $\Omega_{\rm de}$ becomes dominant earlier than the cosmological constant Λ, the two curves come close again at larger a, due to the backreaction from voids, which makes $\rho_{\rm de}$ converge to a cosmological constant. That is, $w_{\rm de}$ converges to −1.

Figure 3 shows the evolution of the effective EOS parameter for ΛCDM and our wCDM model, respectively. The *effective* EOS parameter $w_{\rm eff}(t) = p_{\rm tot}(t)/\rho_{\rm tot}(t)$ is determined by the time-dependent sum of pressures and densities of all cosmic components. (Generally, if one component dominates strongly over the others, $w_{\rm eff}$ is close to the EOS parameter of that component.) In the top panel with the scale factor on the lower x-axis, we recognize the early radiation-dominated phase, where $w_{\rm eff} = 1/3$ to high accuracy. In terms of cosmic time on a linear x-axis scale in the bottom panel, this phase is so short that it is seen as a vertical bar along the y-axis. Once matter strongly dominates in the Universe, shortly after $a_{\rm eq}$, $w_{\rm eff}$ drops to zero. In the latest phase, when Λ begins to dominate the Universe in ΛCDM, the effective EOS parameter drops to its present-day value of $w_{\rm eff} \sim -0.7$. On the other hand, in the wCDM model, the effective EOS parameter initially decreases more rapidly than in ΛCDM. Only by the time the backreaction from voids comes at play in wCDM does the evolution approach that of ΛCDM, around the present, which can also be seen in the bottom panel of the figure.

In that bottom panel, we also highlight the evolution of the effective EOS parameter $w_{\rm eff}$ in the far future for the two models. We can see that, as of a cosmic time of $t \sim 22$ Gyr, the $w_{\rm eff}$ in both models, ΛCDM and wCDM, will show no significant difference, and $w_{\rm eff}$ will be very close to −1 by the time of $t \sim 28$ Gyr for ΛCDM and $t \sim 31$ Gyr for wCDM. However, while the dominance of Λ as a cosmological constant is attributed to the former, it is the (relic) kinematic effect of the Big Bang via $H_{\rm ini}$ in relation to the initial density, respectively, that is responsible for the dominance of $\rho_{\rm de}$ in the latter model.

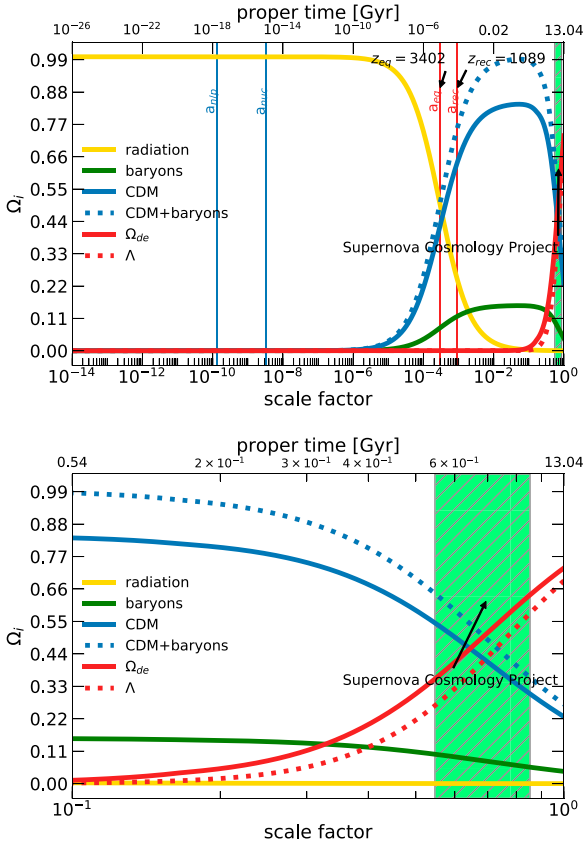

FIGURE 2
Evolution of density parameters in ΛCDM and wCDM. The top panel displays the evolution of the density parameters in the wCDM model vs. scale factor and proper time, respectively. It also includes the Ω_Λ of the ΛCDM model (dotted red curve) in order to compare it to $\Omega_{\rm de}$ (solid red curve) of the wCDM model. Vertical lines are the same as in Figure 1. The bottom panel displays the same quantities but shows a zoom-in to highlight the range of scale factors from $a = 0.1$ to 1. We see that the $\Omega_{\rm de}$ of wCDM becomes dominant earlier than the Ω_Λ of ΛCDM, but that toward $a = 1$, the two curves come closer again. As an illustration, the green-hatched vertical band indicates the range of scale factors of the sample of galaxies used by the Supernova Cosmology Project (Perlmutter et al., 1999). More explanations can be found in the main text.

The present-day value of the expansion rate, the Hubble constant H_0, also differs between the two models: ΛCDM has a value of $H_0 = 67.56$ km/s/Mpc, and wCDM has $H_0 = 72.82$ km/s/Mpc. Of course, the value for ΛCDM is informed by CMB measurements from Planck and is part of the parameters provided by CLASS; see Table 1.

Now, in order to illustrate the late impact by voids onto the expansion history of wCDM, compared to ΛCDM, Figure 5 shows zoom-ins of the evolution of the expansion rate H for $a \geq 10^{-4}$ (top panel) and $a \geq 10^{-1}$ (bottom panel). The vertical red lines indicate the scale factor at matter–radiation equality $a_{\rm eq}$ and at recombination $a_{\rm rec}$, respectively. The solid gray curve at the bottom of each panel displays the relative deviation of H in wCDM from its value in ΛCDM. We can clearly see that at the time of recombination, when the CMB was emitted, there is no difference in H between the models. However, in the late stages of the evolution, the expansion

4.2 Expansion history

Figure 4 shows the expansion history of ΛCDM and wCDM. The top panel displays the growth of the scale factor a with cosmic time t for both models. The bottom panel shows the evolution of the Hubble parameter (i.e., expansion rate) H vs. scale factor a. In wCDM, the scale factor grows faster than in ΛCDM. This results in a younger age of 13.04 Gyr for wCDM than 13.80 Gyr for ΛCDM.

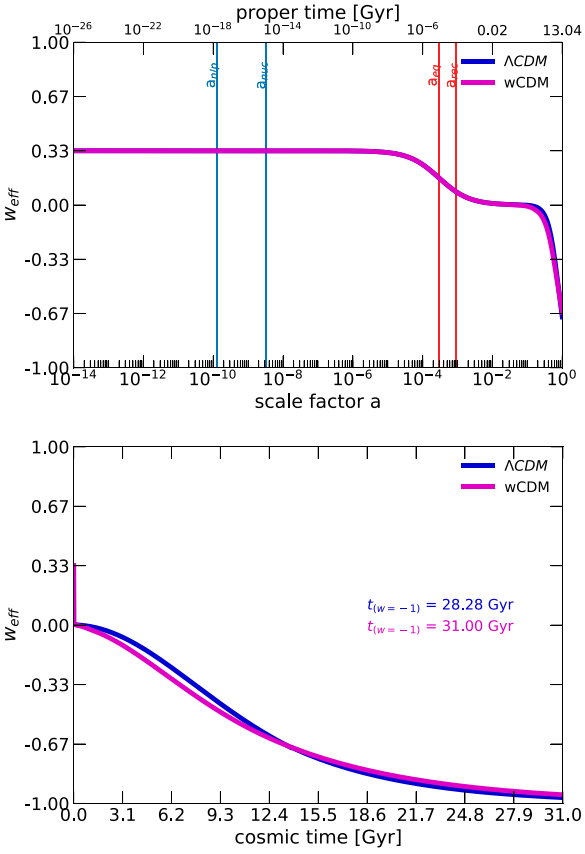

FIGURE 3
Evolution of the effective EOS parameter $\boldsymbol{w}_{\text{eff}}$ in extended and concordance ΛCDM. The top panel displays the evolution of w_{eff} in both models vs. scale factor and proper time, respectively, with the same vertical lines as in Figure 1. The bottom panel displays w_{eff} vs. cosmic time in linear scale. The cosmic time when $w_{\text{eff}} \simeq -1$ is indicated in the plot; it amounts to $t = 28.28$ Gyr for ΛCDM vs. 31.0 Gyr for the ΛCDM extension, respectively.

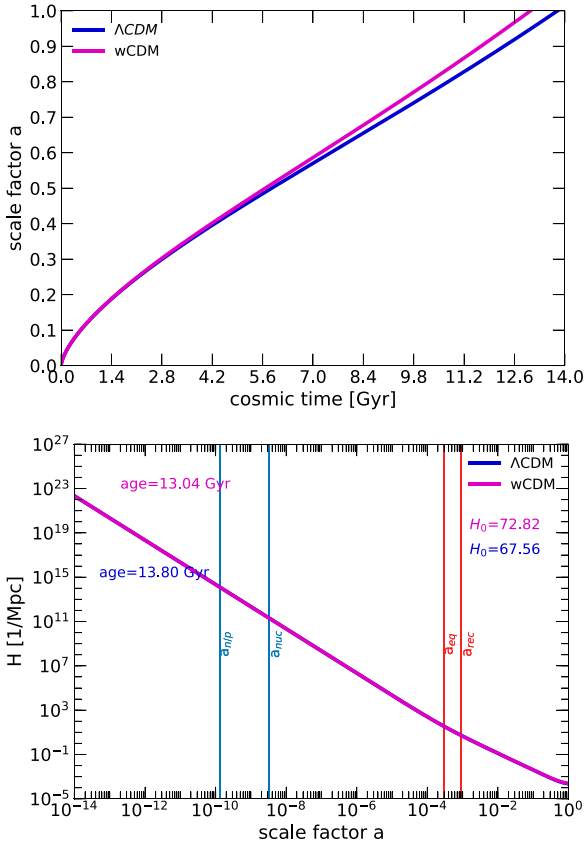

FIGURE 4
Evolution of the scale factor and Hubble parameter in ΛCDM and wCDM. The top panel shows the evolution of the scale factor vs. cosmic time for ΛCDM (blue curve) and wCDM (magenta curve); note the linear scales in this plot. The wCDM model expands faster than the ΛCDM model, which can be better recognized in Figure 5. The bottom panel shows the evolution of the expansion rate or Hubble parameter H (displayed in CLASS conventions in units of 1/Mpc) vs. scale factor for both models. Its present-day value H_0 differs: ΛCDM has $H_0 = 67.56$ km/s/Mpc, whereas wCDM has $H_0 = 72.82$ km/s/Mpc. Vertical lines in the bottom panel are the same as in Figure 1.

rate in the wCDM model increases once the impact of the formation of the cosmic web becomes relevant. At a scale factor of $a \sim 0.8$, the deviation reaches a maximum but then decreases, yielding a value of $H_0 = 72.82$ km/s/Mpc. The bottom panel exemplifies this even more clearly. Again, this shift to a higher value of H_0 by ≈8% is due to the backreaction caused by voids. The origin of the increase of H_0 in our ΛCDM extension is the time-dependence (scale-factor dependence) of the EOS parameter $w_{\text{de}}(a)$. As mentioned earlier, we cannot use the customary procedure applied in ΛCDM to determine the energy density ρ_{de} via Equation 11, as the EOS parameter $w_{\text{de}}(a)$ is no longer a constant. Hence, we must perform a forward-in-time integration of ρ_{de} by integrating Equation 9 to solve the Friedmann Equation 6, which we discussed in detail in Foidl and Rindler-Daller (2024). The consequence of this integration is that, as $w_{\text{de}}(a)$ decreases with time, it leads to an increase in the value for H_0, and this value is higher than the parameterized Planck value given in Table 1. As a result, the ΛCDM extension can explain the Hubble tension problem, on which we elaborate below.

4.3 The Hubble tension and σ_8-tension

Our wCDM model of the previous section is phenomenologically similar to models of quintessence or "early dark energy" (EDE), which also propose solutions to the Hubble tension problem. A review of these models is given in Poulin et al. (2023). Further studies on the Hubble tension include, for example, Dainotti et al. (2022b), Dainotti et al. (2021), Dainotti et al. (2022a), Bargiacchi et al. (2023b), Bargiacchi et al. (2023a), Ó Colgáin et al. (2021), Krishnan et al. (2021), and Benedetto et al. (2021). The Hubble tension problem refers to the reported discrepancy between the values[9] of H_0 derived from measurements of the CMB vs. those derived from measurements

9 Strictly speaking, H_0 refers to H at $z = 0$, but because the community casually uses the notation H_0 also for any H at low $z \lesssim 1$, we stick to this convention.

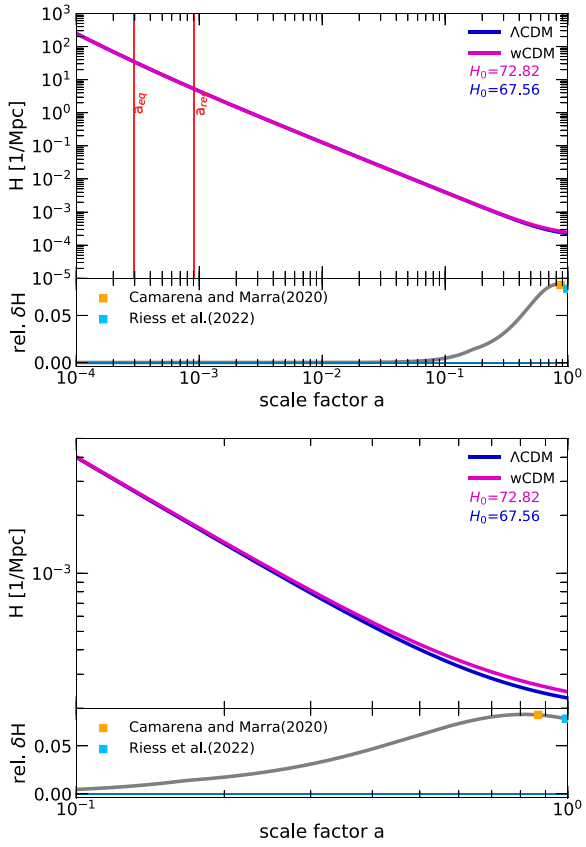

FIGURE 5
Evolution of Hubble parameter vs. scale factor. The top panel shows the evolution of the expansion rate H vs. scale factor for ΛCDM (blue curve) and the ΛCDM extension (magenta curve) and their relative deviation as the gray curve in the bottom of each panel. The panels only differ in the range of scale factors shown. The bottom panel shows that the ΛCDM extension expands faster than ΛCDM. The solid orange and blue squares indicate measurement values of H_0 by Camarena and Marra (2020) and Riess et al. (2022), respectively. The red vertical lines in the top panel are the same as in Figure 1. In our wCDM model, the Hubble parameter H increases by ~8% by the present, compared to that of ΛCDM. As a result, the model explains the Hubble tension problem and agrees with H_0-measurements at different redshifts.

in the "local" Universe, using standard candles such as SNe Ia or Cepheid variables. The measurements in the local Universe consistently reveal a higher value of H_0 than the measurements of the CMB. This problem is discussed, for example, in Di Valentino et al. (2021), where two measurement values in the local Universe are of particular interest to us for a comparison with our ΛCDM extension (see their Figure 1 and the bottom parts of both panels of our Figure 5): Riess et al. (2022) with $H_0 = 73.04$ km/s/Mpc and Camarena and Marra (2020) with $H_0 = 75.4$ km/s/Mpc. The wCDM model, with its value of $H_0 = 72.82$ km/s/Mpc, agrees quite well with the value determined by Riess et al. (2022). The result of Camarena and Marra (2020) seems to be an outlier, as their H_0-value is even higher. The explanation for this can be found in the redshift range of the respective samples of galaxies for these two measurements. The redshifts of the sample used in Riess et al. (2022) lie between $z = 0.011$ and $z = 0.02$, whereas those of the sample in Camarena and Marra (2020) are in a range between $z = 0.023$ and $z = 0.15$. Yet, because wCDM exemplifies a higher value of H around that same epoch, it can also explain the results of Camarena and Marra (2020), whose measurement neatly lies on the maximum of the deviation of H in the wCDM model, compared to ΛCDM; see Figure 5. This result came as quite a surprise when we studied this comparison in detail. Moreover, the data analysis procedure they apply is compatible with the one we proposed in Foidl and Rindler-Daller (2024). This decrease of H in the deviation from its evolution in ΛCDM toward $z = 0$ (after a maximum of deviation) is also reported in Krishnan et al. (2020).

Now, many models that mitigate the Hubble tension predict an increase in the σ_8 tension (see, e.g., Kamionkowski and Riess, 2023), which has emerged in recent years. This is a measure of the homogeneity of the Universe, where S_8 is defined as $\sigma_8\sqrt{\Omega_m/0.3}$, with σ_8 being the standard deviation of the density fluctuation in a sphere of radius 8 h^{-1} Mpc. A disagreement of more than 4σ has been found between the extrapolation of the CMB temperature fluctuations forward to the present day and what is measured by multiple probes of the inhomogeneity in the nearby Universe: The value of S_8 derived from the CMB is higher than that observed in the local Universe. A mitigation of the Hubble tension (i.e., by increasing H_0) increases the σ_8 tension. In Rebouças et al. (2024), this was addressed by assuming a modification of EDE in the late universe, which solves both problems. However, the modifications to EDE are purely empirically motivated, whereas our wCDM model is based upon a consistent set of physical processes involved in the evolution of the Universe.

In addition, we find that our $S_8 = 0.784$ almost exactly matches the value of the DES-Y3 measurements for which $S_8 = 0.782 \pm 0.019$, by assuming a constant neutrino mass $\sum M_\nu$. The final data release by the Planck mission in Tristram et al. (2024) also compares their result to this value. The result is in agreement with the findings by Rebouças et al. (2024), who found that a time-dependent $w(z)$ at late times can resolve Hubble tension *and* σ_8-tension. Indeed, this is the case in our extension wCDM because the evolution of $w(z)$ in our model is constant in the early Universe, but in the late stages, it becomes a time-dependent function.

Now, to investigate whether the lower age of the wCDM model constitutes a problem, we compare some age indicators from the literature, notably estimates for the ages of the oldest known stars in the Universe. Their ages are estimated basically via two different methods: the abundance of heavy elements, mainly those formed by the r-process in core collapse supernovae; the second is the determination of the time of the main sequence turn-off of metal-poor stars in globular clusters. A short review of methods and observations is given in Weinberg (2008), with age estimates of the oldest stars between 11.5–14 Gyr, where the error bars are ~2 Gyr. The observations of metal-poor galaxies by Grebel (2012) and globular clusters in the local Universe by Grebel (2016) display consistent results, albeit with larger error bars of 2 – 4 Gyr. A more recent observation, based on the age of the metal-poor globular cluster NGC 6397 using WFC3/IR photometry, is given in Correnti et al. (2018), showing a similar age range with smaller error bars of 12.6 ± 0.7 Gyr. All these results are consistent with the age of our wCDM model.

For comparison's sake, we also computed the age of a ΛCDM universe using H_0 from Riess et al. (2022), while keeping the other

parameters unchanged: the result is 12.50 Gyr. This age for ΛCDM would also still be on the safe side with respect to the age estimates of the oldest known stars.

Cimatti and Moresco (2023) follow a different approach. They select the oldest objects from the literature and perform a statistical analysis within a ΛCDM cosmology to determine the upper limit of H_0 compatible with the ages of the selected objects. They find $H_0 < 73.0 \pm 2.5$ km/s/Mpc with a probability of 93.2%. So, the "Riess model" is also within these constraints. Because the expansion rate in wCDM increases only later in time, it is less affected by this upper limit.

Let us also comment on the early galaxies that have been found recently by the James Webb Space Telescope; see Curtis-Lake et al. (2023), Finkelstein et al. (2023), and Robertson et al. (2023). It has been estimated that these galaxies have formed only approximately 320 million years after the Big Bang. However, we stress that such estimates require the adoption of a specific cosmological model to convert the measured redshifts into an age. Adopting a ΛCDM model with the H_0 determined by the Planck telescope, or the H_0 determined from the local Universe (e.g., by Riess et al. (2022)), will in each case shift the age of the galaxies accordingly, and the same is true if we adopt the wCDM model instead. In each case, there is no conflict between the ages of these model universes and those of the early galaxies.[10]

Recent studies by, for example, Dainotti et al. (2022b), Dainotti et al. (2021), Dainotti et al. (2022a), Bargiacchi et al. (2023b), Bargiacchi et al. (2023a), Ó Colgáin et al. (2021), and Krishnan et al. (2021), indicate that the evolution of the expansion rate H at low redshift is in conflict with the assumption of a cosmological constant, and DDE models seem to be preferred. These results may indicate that the origin of the Hubble tension is likely to be in cosmology and not in local measurement issues (e.g., Krishnan et al., 2021), as observations with increasing accuracy of H_0 in the local Universe seem to exacerbate the Hubble tension (e.g., Dainotti et al., 2023; Khalife et al., 2024). The evolution of the expansion rate, shown in Figure 5, displays a peak in the deviation to ΛCDM at $a \sim 0.8$. In fact, the position of this peak seems to be characteristic of individual DE candidates; see Foidl and Rindler-Daller (2024).

5 Results for the owCDM extension to ΛCDM

First, we discuss the temperature spectrum of our wCDM model compared to the ΛCDM concordance model. In CLASS, we can readily incorporate the equations for wCDM in both the background module and in the perturbation module, in order to calculate perturbation spectra. As already mentioned in the previous section, CLASS has been proven to be in conformance with the Planck results within a level of 0.01%. Hence, we can test our model by comparison to the temperature spectrum of the ΛCDM concordance model computed with CLASS, without the need for a full Markov chain Monte Carlo (MCMC) data analysis starting with CMB raw data.

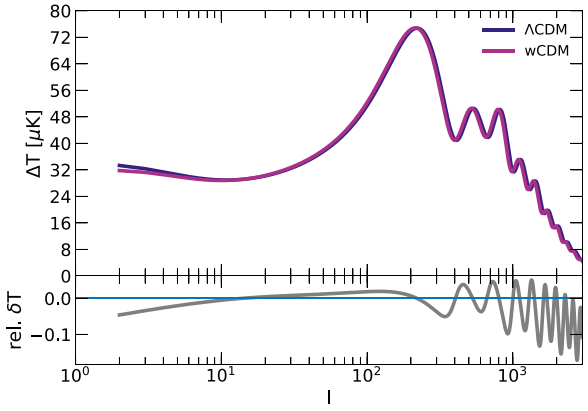

FIGURE 6
CMB temperature power spectrum in ΛCDM (blue) and in our wCDM model (magenta). The relative differences are shown at the bottom of the panel and amount to ~15%.

The parameter set, used in the computation of the CMB temperature spectrum of wCDM, is the same as in Section 4, Table 1. It is based upon the standard CDM framework, concerning its matter content and the cosmic web (and void) structure. Therefore, we expect no big differences in the perturbation spectra between wCDM and concordance ΛCDM. In fact, the output by CLASS confirms this expectation. Figure 6 shows the power spectrum of the CMB temperature anisotropies of the wCDM and the ΛCDM model.

Although we see no significant differences in the structure of the peaks in the CMB temperature power spectrum, the deviations are at a $\lesssim 15\%$ level. The peak structure is almost identical, but the peaks are slightly shifted to the left, which can be explained as follows. The amplitudes of the peaks in the spectrum are determined by the density parameters $\Omega_{r,0}$ for radiation and $\Omega_{b,0}$ and $\Omega_{\mathrm{CDM},0}$ for the matter components. The relative height of the peaks is determined by the ratio of $\Omega_{b,0}$ and $\Omega_{\mathrm{CDM},0}$. Hence, it is obvious that the structure of the peaks agrees with ΛCDM, as we used the concordance values for these density parameters. However, the parameterization of DE impacts the expansion rate, as exemplified in Section 4.2. Because there is no interaction between DE and the other cosmic components, the replacement of DE for Λ does not impact the structure of the peaks. Keeping in mind that the multipole moments, shown on the x-axis, are in Fourier space, however, explains the shift of the spectrum to the left-hand side. More precisely, it is not a shift, but rather a stretching (compressing) of the spectrum from the right-hand side to the left-hand side, with increasing (decreasing) expansion rate. Thus, the slightly higher value of H_0 of wCDM (see Figure 5), compared to ΛCDM, explains the minor shift to the left, while providing a solution to the Hubble tension.

Remember that the cosmological parameter $\Omega_{k,0}$ for the spatial curvature has an analogous impact on the spectrum, shifting the spectrum while the structure of the peaks remains unchanged. This degeneracy in the effect on the spectrum between a change of spatial curvature and dark energy is well known (see, e.g., Hu and Dodelson, 2002) and quite obvious. Both components do not interact with matter or radiation, but the expansion history (i.e., H_0)

10 Or, rephrased, all these cosmological models face a potential challenge in explaining the early formation of these galaxies.

is affected. While there is no impact on the structure of the peaks, a shift of the peaks occurs.

In Foidl and Rindler-Daller (2025), we argued that the free-falling, comoving FLRW observer resides in a local inertial frame, where special relativity applies and therefore, the observer perceives flat space. In the FLRW metric, the FLRW observer moves with freely streaming particles, which represent the galaxies in the Universe. The expansion of the temperature power spectrum into spherical harmonics to display these measurement results does not include the first multipole moment (see Figure 6), the dipole, for practical purposes. The dipole moment is induced by our peculiar motion against the CMB, and it is subtracted from the CMB raw data because its amplitude of the order of 10^{-3} K would strongly dominate the actual signal of interest—the temperature fluctuations, of order 10^{-5} K, sourced in the early Universe. However, the fact that the dipole moment is still small, compared to the mean, simply confirms that we—as observers here—fulfill the criterion of being comoving FLRW observers, not strictly (Peacock, 1999) but to a very high degree (a well-known fact, but see also, for example, von Hausegger (2024)). Indeed, this observational finding of a small dipole actually confirms that we comove with the expansion to a high degree. So, the metric we perceive is very close to the flat Minkowski metric.

The dipole, which corresponds to our peculiar motion against the CMB, offsets us from the perfectly comoving FLRW observer, who observes a perfectly flat space. Consequently, we now expand the scope and take into account our peculiar motion relative to the CMB, caused by our "local" cosmological environment (see, e.g., Tully et al., 2014), considering the spatial curvature Ω_k (because $\Omega_k = 0$ only applies to the perfectly comoving FLRW observer).

Therefore, we fit the parameters $\Omega_{k,0}$ and $\Omega_{\mathrm{de},0}$ (the other parameters remain unchanged as they are not impacted by the dipole moment and are the same as for wCDM and ΛCDM) of our model to the ΛCDM CMB spectrum as well as to the value $H_0 = 73.04$ km/s/Mpc, derived by Riess et al. (2022). As is customary, we call the resulting model owCDM model.[11] Because we focus on the reasoning of the conception of our owCDM model, we used this simple proof-of-concept procedure. Otherwise, an MCMC analysis including all parameters of the model would be preferred. The results are depicted in Figure 7.

Now, the deviation from the ΛCDM spectrum amounts to a $\lesssim 0.01\%$ level (disregarding the higher deviations at small l, where the error bars in the actual CMB measurements are larger anyway). We find a spatial curvature of $\Omega_{k,0} = -0.0197$ that describes a local effect, induced by our "local" attractive cosmic environment, decoupling us from perfect Hubble flow (see Tully et al., 2014). This value is compatible with the final PR4 of the Planck mission (Tristram et al., 2024) with $\Omega_{k,0} = -0.012 \pm 0.010$. In addition, we find for the owCDM model $S_8 = 0.798$, which is within 1σ with DES-Y3's result of $S_8 = 0.782 \pm 0.019$.

To reiterate, we stress that the evolution of w_{de} with cosmic time and the spatial curvature $\Omega_{k,0} = -0.0197$ are both effects of the nonlinear structure formation. The time-dependence of w_{de} is a global effect by the voids dominating the volume of the Universe, whereas $\Omega_{k,0} = -0.0197$ is a local effect by our local attractive cosmic environment, decoupling us from perfect Hubble flow.

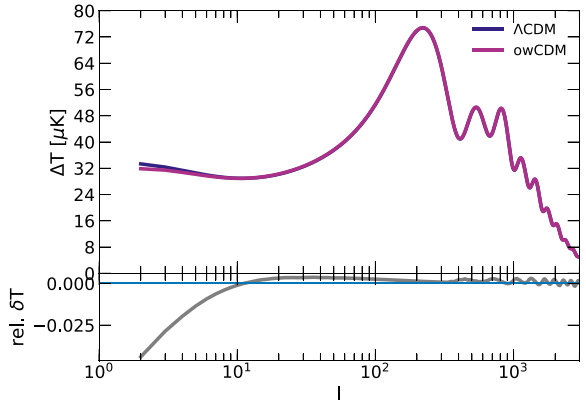

FIGURE 7
CMB temperature power spectrum in ΛCDM (blue) and in our owCDM model (magenta). The relative differences are shown at the bottom of the panel and amount to ~0.01%.

6 Summary and discussion

Based on our proposal of Foidl and Rindler-Daller (2025), we presented two extensions to ΛCDM, wCDM, and owCDM, which propose solutions to the Hubble tension, explain the spatial curvature as reported by Planck PR4 (Tristram et al., 2024), and include the following additional novelties:

a. Customarily, the averaging problem only considers the density of (linear and nonlinear) perturbations and finds that there is no significant backreaction onto the evolution of the background universe. We additionally consider the volume of perturbations and find a mild backreaction, caused by voids dominating the volume of the Universe. The initially constant EOS parameter, $w_{\mathrm{de}} \simeq -0.8$, evolves to a more negative value of $w_{\mathrm{de}} \simeq -0.9$ at the present time, once the impact by voids has become significant. While this impact by voids onto the expansion history affects an overall change of only approximately 8% in the expansion rate of the late Universe, it is enough for our wCDM model to explain the Hubble tension problem, which refers to the offset between measurements of the Hubble constant H_0, using the CMB versus standard candles in the "local" Universe.
b. In owCDM, we include the effect of the CMB dipole, which is otherwise not included in the calculations of FLRW models. This explains the curvature of space measured by PR4 of the Planck mission (Tristram et al., 2024) as the mere effect of our peculiar motion against the CMB, which "decouples" us from the Hubble flow.

We would like to note that we presented two extensions to ΛCDM, which are based on a time-dependent evolution of the EOS parameter $w_{\mathrm{de}}(z)$ of a kinematically explained "DE component."

11 This acronym is customarily used for extensions to ΛCDM, when $w(z)$ is different from –1 and additionally a spatial curvature is applied; see, for example, Particle Data Group Review Chapter 28 Dark Energy Group et al. (2022).

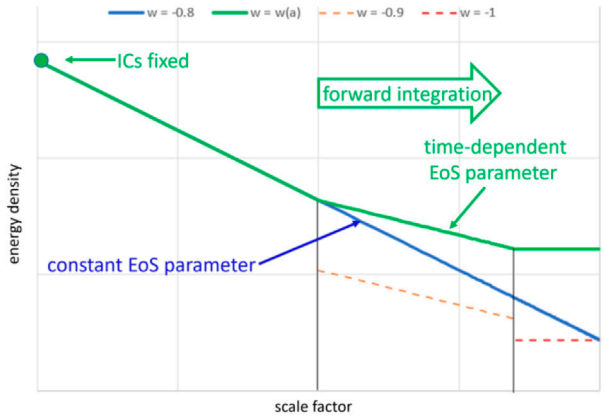

FIGURE 8
Illustrative comparison between the evolution of energy density for a cosmic component with a constant or nonconstant EOS (arbitrary scaling). The blue component has a constant EOS parameter $w = -0.8$. The green component has a nonconstant EOS parameter w, which starts with $w = -0.8$ (equal to the blue component) and evolves in two steps (indicated by the solid vertical black lines) to $w = -0.9$ (the slope is indicated by the dashed orange line) and finally to $w = -1$ (the slope is indicated by the dashed red line). The final density at the present time is higher for the green component (Reproduced Figure 2 of Foidl and Rindler-Daller (2024)).

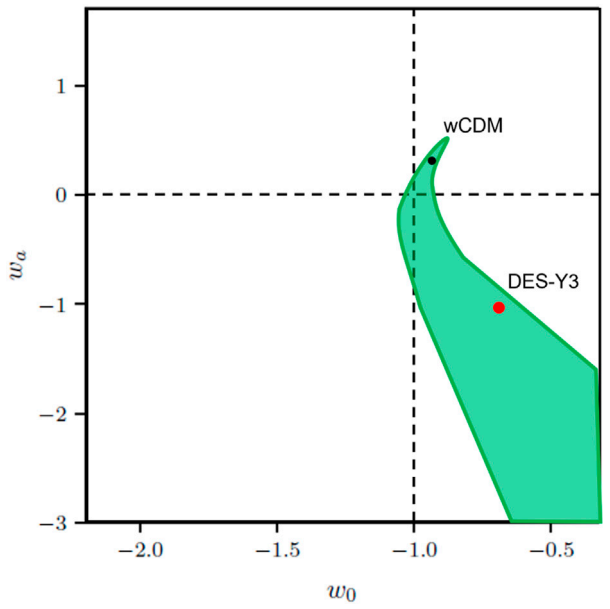

FIGURE 9
Illustration of the degeneracy in the CPL plane. The green region depicts schematically (based on exemplary computations of models of previous literature) the w_0-w_a-pairs in the CPL plane, giving Planck-like results for H_0 and the power spectra. The solid black circle represents the results of our wCDM model. The orange circle depicts the results of DES-Y3. The intersection of the dashed lines indicates the cosmological constant $(w_0, w_a) = (-1, 0)$.

In contrast to other parameterizations, like the empirically defined CPL parameterization, we conceived our DE model based on well-accepted concepts and theories, already applied in ΛCDM. Furthermore, our extensions wCDM and owCDM can be tested using ongoing and future observational campaigns within their current scope. Only minor adaptation to the process of data analysis is required to implement our extensions into these campaigns, as we also exemplified in Foidl and Rindler-Daller (2024), where we present a list of observational programs of interest. By determining the EOS of DE, these programs will be able to rule out our extensions or confirm them by providing an even more accurate update of our function of $w_{\rm de}(z)$, that is, a more observationally informed EOS, compared to our approximations, based on the Millennium simulation, in this article.

Observations indicate that the evolution of the expansion rate H at low redshift contradicts the assumption of a cosmological constant and that dynamical DE models with a time-dependent EOS parameter may be preferable; see, for example, Dainotti et al. (2022b), Dainotti et al. (2021), Dainotti et al. (2022a), Bargiacchi et al. (2023b), Bargiacchi et al. (2023a), Ó Colgáin et al. (2021), and Krishnan et al. (2021). These results may indicate that the origin of the Hubble tension is likely to be in cosmology and not in local measurement issues, which we discussed in detail in Foidl and Rindler-Daller (2024).

Also, in that article, we find that the Hubble tension problem can be explained phenomenologically in a very natural way by a DE component with a decreasing EOS parameter $w(z)$. In particular, the EOS parameter $w(z)$ evolves from −0.8 in the early Universe to −0.9 at the present. Our ΛCDM extensions described in this article fulfill exactly this property. Moreover, our results are in very good agreement in the CPL plane with data from baryon acoustic oscillations (BAO) and redshift-space distortion (RSD) measurements from the eBOSS, 6dF, and MGS galaxy surveys (Alam et al., 2021) (see the green contours in Figure 5 of Dark Energy Survey Year 3 (DES-Y3) results (Abbott et al., 2023)).

On the other hand, we realize that our result does not agree with the overall DES-Y3 results for their wCDM model. Their result in the CPL plane shows values of $w_0 = -0.95^{+0.08}_{-0.08}$ and $w_a = -0.4^{+0.4}_{-0.3}$, which is an increasing EOS parameter $w(z)$, in contrast to our decreasing EOS parameter $w(z)$. Similarly, the latest results from the Dark Energy Spectroscopic Instrument (DESI) survey (Adame et al., 2025) report (in combination with PantheonPlus) $w_0 = -0.827 \pm 0.063$ and $w_a = -0.75^{+0.29}_{-0.25}$, again indicating an increasing EOS parameter $w(z)$. These increasing DDE models start in the early Universe as phantom energy and later cross the phantom line "−1" to a present value above −1. However, these results are consistent with the results of the Planck 2018 Planck-Collaboration (2020a) for the wCDM alternative to ΛCDM.

In Foidl and Rindler-Daller (2024), we showed that the phantom-energy-type DDE model of DES-Y3 perfectly reproduces the ΛCDM results for the power spectra and expansion history, including the Planck-based value for H_0 (see Figures 7, 8 in Foidl and Rindler-Daller (2024)). However, these results are not compatible with measurements of H_0 in the local Universe (e.g., Riess et al., 2022), which we discuss in detail in Foidl and Rindler-Daller (2024).

From the perspective of Foidl and Rindler-Daller (2024), we explain these results by the fact that the data analysis method used in these campaigns is trapped in the degeneracy of DDE models with a time-dependent EOS parameter in the CPL plane. The reason for this is illustrated in Figure 2 of Foidl and Rindler-Daller (2024). There, we compare a DDE model and a model with a constant

EOS parameter, both of course with identical initial conditions. The result is that due to the decreasing EOS parameter, the value for H_0 is higher than in the model with a constant EOS parameter. Because this is our main argument for the different results compared to Planck, DES, and DESI, we present it again here as Figure 8, for the convenience of the reader. The reason for this is that a decreasing EOS parameter leads to less deceleration in the late stages of the evolution and thus to an increased value of H_0. Similarly, an increasing EOS parameter leads to stronger deceleration and thus a lower value of H_0.

Figure 9 shows the region in the CPL plane that yields Planck-like results for H_0 and the power spectra for probably an infinite number of DDE models (discussed in Foidl and Rindler-Daller (2024)). Planck, DES, and DESI use very similar data analysis procedures, for example, MCMC methods, and even apply the same set of tools in their data analysis. In Foidl and Rindler-Daller (2024), we discussed that these tools and methods carry the risk of inadvertently restricting the priors of H_0 in the MCMC analysis, which can significantly bias the results.

To conclude the discussion, we focus on the physics of the Friedmann (Equation 6) in the late stages of evolution, where Λ or DE, respectively, dominates the energy density of the Universe. The DDE models reported by Planck-Collaboration (2020b), DES (Abbott et al., 2023), and DESI (Adame et al., 2025) begin in the early Universe as phantom energy with an increasing EOS parameter, such that they cross the phantom line "−1" (e.g., DESI at $z \simeq 0.45$) well before they become the dominant component in the Universe. Prior to this point in time, DE is sub-dominant by many orders of magnitude (phantom energy even many orders of magnitude more than the cosmological constant) and has no impact on the expansion history of the Universe. The Nobel Prize-winning measurements of Perlmutter et al. (1999), Schmidt et al. (1998), and Riess et al. (1998) revealed the accelerating expansion of the Universe by directly measuring the *decreasing* deceleration in the late stages of the Universe's expansion. These direct measurements were insensitive to the peculiarities of a cosmological model. However, an increasing EOS parameter of the DE component implies an *increasing* deceleration as the contributions of the other components to the expansion history are sub-dominant (e.g., for DESI w_{de} evolving from −1 to $w_{de} = -0.827$ because $z \simeq 0.45$), which is inconsistent with the observation of a late-time accelerated expansion. Therefore, we emphasize that DDE models with an increasing EOS parameter (in the CPL parametrization) are incompatible with the late-time accelerated expansion of the Universe. Furthermore, our extended MCMC procedure, proposed in Foidl and Rindler-Daller (2024), also excludes DDE models with an increasing EOS parameter. In contrast, our ΛCDM extensions with a decreasing EOS parameter (w_{de} evolving from −0.8 to $w_{de} = -0.9$ and asymptotically converging toward −1 in the future) are consistent with the phenomenology of a late-time accelerated expansion and provide a possible solution to the Hubble tension in a very natural way.

Our owCDM model is probably not the final answer to DE and the Hubble tension because we derived the parametrization of the DDE component from simple approximations and the results of the Millennium simulation. It could be seen as a first step in a promising direction. Future observations will provide a more accurate (i.e., a more observationally informed) update of our function of $w_{\rm de}(z)$ and falsify or confirm our approach.

Data availability statement

The original contributions presented in the study are included in the article/supplementary material, further inquiries can be directed to the corresponding authors.

Author contributions

HF: Software, Conceptualization, Writing – original draft, Visualization, Writing – review and editing, Investigation, Methodology. TR-D: Supervision, Writing – review and editing, Funding acquisition, Writing – original draft, Formal Analysis.

Funding

The author(s) declared that financial support was received for this work and/or its publication. TR-D acknowledges the support by the Austrian Science Fund (FWF) through the FWF Single-Investigator Grant (FWF-Einzelprojekt) No. P36331-N and the hospitality of the Wolfgang Pauli Institute.

Acknowledgements

The authors are grateful to Glenn van de Ven, Paul Shapiro, Dragan Huterer, Oliver Hahn, and Bodo Ziegler for helpful and valuable discussions, concerning an earlier version of this manuscript.

Conflict of interest

The author(s) declared that this work was conducted in the absence of any commercial or financial relationships that could be construed as a potential conflict of interest.

Generative AI statement

The author(s) declared that generative AI was not used in the creation of this manuscript.

Any alternative text (alt text) provided alongside figures in this article has been generated by Frontiers with the support of artificial intelligence and reasonable efforts have been made to ensure accuracy, including review by the authors wherever possible. If you identify any issues, please contact us.

Publisher's note

References

Abbott, T. M. C., Aguena, M., Alarcon, A., Allam, S., Alves, O., Amon, A., et al. (2022). Dark energy survey year 3 results: cosmological constraints from galaxy clustering and weak lensing. *Phys. Rev. D.* 105, 023520. doi:10.1103/PhysRevD.105.023520

Abbott, T. M. C., Aguena, M., Alarcon, A., Alves, O., Amon, A., Andrade-Oliveira, F., et al. (2023). Dark energy survey year 3 results: constraints on extensions to ΛCDM with weak lensing and galaxy clustering. *Phys. Rev. D.* 107, 083504. doi:10.1103/PhysRevD.107.083504

Adame, A. G., Aguilar, J., Ahlen, S., Alam, S., Alexander, D. M., Alvarez, M., et al. (2025). DESI 2024 VI: cosmological constraints from the measurements of baryon acoustic oscillations. *J. Cosmol. Astropart. Phys.* 2025, 021. doi:10.1088/1475-7516/2025/02/021

Alam, S., Aubert, M., Avila, S., Balland, C., Bautista, J. E., Bershady, M. A., et al. (2021). Completed SDSS-IV extended baryon oscillation spectroscopic survey: cosmological implications from two decades of spectroscopic surveys at the apache point observatory. *Phys. Rev. D.* 103, 083533. doi:10.1103/PhysRevD.103.083533

Amendola, L., and Tsujikawa, S. (2010). *Dark energy*. Cambridge University Press.

Barausse, E., Matarrese, S., and Riotto, A. (2005). Effect of inhomogeneities on the luminosity distance-redshift relation: is dark energy necessary in a perturbed universe? *Phys. Rev. D.* 71, 063537. doi:10.1103/PhysRevD.71.063537

Bargiacchi, G., Dainotti, M. G., and Capozziello, S. (2023a). Tensions with the flat ΛCDM model from high-redshift cosmography. *MNRAS* 525, 3104–3116. doi:10.1093/mnras/stad2326

Bargiacchi, G., Dainotti, M. G., Nagataki, S., and Capozziello, S. (2023b). Gamma-ray bursts, quasars, baryonic acoustic oscillations, and supernovae ia: new statistical insights and cosmological constraints. *MNRAS* 521, 3909–3924. doi:10.1093/mnras/stad763

Benedetto, E., Feoli, A., and Iannella, A. L. (2021). A determination of the $\Omega_{0m}h^2$ cosmological parameter without tension. *Mod. Phys. Lett. A* 36, 2150157–2150158. doi:10.1142/S0217732321501571

Birkhoff, G. D., and Langer, R. E. (1923). *Relativity and modern physics*. Harvard University Press.

Bondi, H. (1947). Spherically symmetrical models in general relativity. *MNRAS* 107, 410–425. doi:10.1093/mnras/107.5-6.410

Buchert, T. (2000). On average properties of inhomogeneous fluids in general relativity: dust cosmologies. *General Relativ. Gravit.* 32, 105–126. doi:10.1023/A:1001800617177

Buchert, T. (2001). On average properties of inhomogeneous fluids in general relativity: perfect fluid cosmologies. *General Relativ. Gravit.* 33, 1381–1405. doi:10.1023/A:1012061725841

Buchert, T. (2011). Toward physical cosmology: focus on inhomogeneous geometry and its non-perturbative effects. *Class. Quantum Gravity* 28, 164007. doi:10.1088/0264-9381/28/16/164007

Buchert, T., and Ehlers, J. (1997). Averaging inhomogeneous Newtonian cosmologies. *A&A* 320, 1–7. doi:10.48550/arXiv.astro-ph/9510056

Buchert, T., Carfora, M., Ellis, G. F. R., Kolb, E. W., MacCallum, M. A. H., Ostrowski, J. J., et al. (2015). Is there proof that backreaction of inhomogeneities is irrelevant in cosmology? *Class. Quantum Gravity* 32, 215021. doi:10.1088/0264-9381/32/21/215021

Calzetta, E. A., Hu, B. L., and Mazzitelli, F. D. (2001). Coarse-grained effective action and renormalization group theory in semiclassical gravity and cosmology. *Phys. Rep.* 352, 459–520. doi:10.1016/S0370-1573(01)00043-6

Camarena, D., and Marra, V. (2020). Local determination of the Hubble constant and the deceleration parameter. *Phys. Rev. Res.* 2, 013028. doi:10.1103/PhysRevResearch.2.013028

Carloni, S., Leach, J. A., Capozziello, S., and Dunsby, P. K. S. (2008). Cosmological dynamics of scalar tensor gravity. *Class. Quantum Gravity* 25, 035008. doi:10.1088/0264-9381/25/3/035008

Cautun, M., van de Weygaert, R., Jones, B. J. T., and Frenk, C. S. (2014). Evolution of the cosmic web. *MNRAS* 441, 2923–2973. doi:10.1093/mnras/stu768

Chevallier, M., and Polarski, D. (2001). Accelerating universes with scaling dark matter. *Int. J. Mod. Phys. D* 10, 213–223. doi:10.1142/S0218271801000822

Cimatti, A., and Moresco, M. (2023). Revisiting the oldest stars as cosmological probes: new constraints on the Hubble constant. *ApJ* 953, 149. doi:10.3847/1538-4357/ace439

Colberg, J. M., Sheth, R. K., Diaferio, A., Gao, L., and Yoshida, N. (2005). Voids in a ΛCDM universe. *MNRAS* 360, 216–226. doi:10.1111/j.1365-2966.2005.09064.x

Correnti, M., Gennaro, M., Kalirai, J. S., Cohen, R. E., and Brown, T. M. (2018). The age of the old metal-poor globular cluster NGC 6397 using WFC3/IR photometry. *ApJ* 864, 147. doi:10.3847/1538-4357/aad805

Curtis-Lake, E., Carniani, S., Cameron, A., Charlot, S., Jakobsen, P., Maiolino, R., et al. (2023). Spectroscopic confirmation of four metal-poor galaxies at z = 10.3-13.2. *Nat. Astron.* 7, 622–632. doi:10.1038/s41550-023-01918-w

Dainotti, M. G., De Simone, B., Schiavone, T., Montani, G., Rinaldi, E., and Lambiase, G. (2021). On the Hubble constant tension in the SNe Ia pantheon sample. *ApJ* 912, 150. doi:10.3847/1538-4357/abeb73

Dainotti, M. G., De Simone, B. D., Schiavone, T., Montani, G., Rinaldi, E., Lambiase, G., et al. (2022a). On the evolution of the Hubble constant with the SNe Ia pantheon sample and baryon acoustic oscillations: a feasibility study for GRB-cosmology in 2030. *Galaxies* 10, 24. doi:10.3390/galaxies10010024

Dainotti, M. G., Nielson, V., Sarracino, G., Rinaldi, E., Nagataki, S., Capozziello, S., et al. (2022b). Optical and X-ray GRB fundamental planes as cosmological distance indicators. *MNRAS* 514, 1828–1856. doi:10.1093/mnras/stac1141

Dainotti, M. G., Bargiacchi, G., Bogdan, M., Capozziello, S., and Nagataki, S. (2023). Reduced uncertainties up to 43% on the Hubble constant and the matter density with the SNe Ia with a new statistical analysis. *arXiv E-Prints , arXiv:2303.06974*. doi:10.48550/arXiv.2303.06974

de Bernardis, P., Ade, P. A. R., Bock, J. J., Bond, J. R., Borrill, J., Boscaleri, A., et al. (2000). A flat universe from high-resolution maps of the cosmic microwave background radiation. *Nature* 404, 955–959. doi:10.1038/35010035

Di Valentino, E., Mena, O., Pan, S., Visinelli, L., Yang, W., Melchiorri, A., et al. (2021). In the realm of the Hubble tension-a review of solutions. *Class. Quantum Gravity* 38, 153001. doi:10.1088/1361-6382/ac086d

Dinda, B. R. (2023). Exploring the influence of cosmic curvature on large-scale structure formation: part i – homogeneous dark energy presence. *arXiv E-Prints*. arXiv:2312.01393. doi:10.48550/arXiv.2312.01393

Ellis, G. F. R. (1983). "Relativistic cosmology: its nature, aims and problems,". *General relativity and gravitation*. Editors B. Bertotti, F. de Felice, and A. Pascolini, 1, 668.

Finkelstein, S. L., Bagley, M. B., Ferguson, H. C., Wilkins, S. M., Kartaltepe, J. S., Papovich, C., et al. (2023). Ceers key paper. i. an early look into the first 500 myr of galaxy formation with JWST. *ApJ* 946, L13. doi:10.3847/2041-8213/acade4

Flanagan, É. É. (2005). Can superhorizon perturbations drive the acceleration of the universe? *Phys. Rev. D.* 71, 103521. doi:10.1103/PhysRevD.71.103521

Foidl, H., and Rindler-Daller, T. (2024). A proposal to improve the accuracy of cosmological observables and address the Hubble tension problem. *A&A* 686, A210. (Paper I). doi:10.1051/0004-6361/202348955

Foidl, H., and Rindler-Daller, T. (2025). The importance of GR's principle of equivalence for kinematically determined Friedmann-Lemaitre-Robertson-Walker universes. *Front. Astronomy Space Sci.* 12, 1627777. (Paper II). doi:10.3389/fspas.2025.1627777

Friedmann, A. (1922). Über die Krümmung des Raumes. *Z. fur Phys.* 10, 377–386. doi:10.1007/BF01332580

Gasperini, M., Marozzi, G., and Veneziano, G. (2009). Gauge invariant averages for the cosmological backreaction. *J. Cosmol. Astropart. Phys.* 2009, 011. doi:10.1088/1475-7516/2009/03/011

Geshnizjani, G., Chung, D. J., and Afshordi, N. (2005). Do large-scale inhomogeneities explain away dark energy? *Phys. Rev. D.* 72, 023517. doi:10.1103/PhysRevD.72.023517

Grebel, E. K. (2012). "Metal-poor galaxies in the local universe," in *First stars IV - from Hayashi to the future*. Editors M. Umemura, and K. Omukai (American Institute of Physics Conference Series), 1480, 172–183. doi:10.1063/1.4754351

Grebel, E. K. (2016). "Globular clusters in the local group,". *Star clusters and black holes in galaxies across cosmic time*. Editors Y. Meiron, S. Li, F. K. Liu, and R. Spurzem, 312, 157–170. doi:10.1017/S1743921315008078

Group, P. D., Workman, R. L., Burkert, V. D., Crede, V., Klempt, E., Thoma, U., et al. (2022). Review of particle physics. *Prog. Theor. Exp. Phys.* 2022, 083C01. doi:10.1093/ptep/ptac097

Gruzinov, A., Kleban, M., Porrati, M., and Redi, M. (2006). Gravitational backreaction of matter inhomogeneities. *J. Cosmol. Astropart. Phys.* 2006, 001. doi:10.1088/1475-7516/2006/12/001

Guth, A. H. (1981). Inflationary universe: a possible solution to the horizon and flatness problems. *Phys. Rev. D.* 23, 347–356. doi:10.1103/PhysRevD.23.347

Hinshaw, G., Larson, D., Komatsu, E., Spergel, D. N., Bennett, C. L., Dunkley, J., et al. (2013). Nine-year Wilkinson microwave anisotropy probe (WMAP) observations: cosmological parameter results. *ApJS* 208, 19. doi:10.1088/0067-0049/208/2/19

Hirata, C. M., and Seljak, U. (2005). Can superhorizon cosmological perturbations explain the acceleration of the universe? *Phys. Rev. D.* 72, 083501. doi:10.1103/PhysRevD.72.083501

Hogg, D. W., Eisenstein, D. J., Blanton, M. R., Bahcall, N. A., Brinkmann, J., Gunn, J. E., et al. (2005). Cosmic homogeneity demonstrated with luminous red galaxies. *ApJ* 624, 54–58. doi:10.1086/429084

Hu, W., and Dodelson, S. (2002). Cosmic microwave background anisotropies. *ARA&A* 40, 171–216. doi:10.1146/annurev.astro.40.060401.093926

Icke, V. (1984). Voids and filaments. *MNRAS* 206, 1P–3P. doi:10.1093/mnras/206.1.1P

Icke, V. (2001). "Correlations in a random universe," in *Historical development of modern cosmology*. Editors V. J. Martínez, V. Trimble, and M. J. Pons-Bordería (San Francisco: Astronomical Society of the Pacific), 252, 337.

Icke, V., and van de Weygaert, R. (1987). Fragmenting the universe. *A&A* 184, 16–32.

Icke, V., and van de Weygaert, R. (1991). The galaxy distribution as a Voronoi foam. *QJRAS* 32, 85–112.

Jebsen, J. T. (1921). On the general spherically symmetric solutions of Einstein's gravitational equations *in vacuo*. *Arkiv Matematik, Astronomi Och Fysik* 15, 18.

Kamionkowski, M., and Riess, A. G. (2023). The Hubble tension and early dark energy. *Annu. Rev. Nucl. Part. Sci.* 73, 153–180. doi:10.1146/annurev-nucl-111422-024107

Khalife, A. R., Zanjani, M. B., Galli, S., Günther, S., Lesgourgues, J., and Benabed, K. (2024). Review of Hubble tension solutions with new SH0ES and SPT-3G data. *J. Cosmol. Astropart. Phys.* 2024, 059. doi:10.1088/1475-7516/2024/04/059

Koksbang, S. M. (2021). Searching for signals of inhomogeneity using multiple probes of the cosmic expansion rate H(z). *Phys. Rev. Lett.* 126, 231101. doi:10.1103/PhysRevLett.126.231101

Koksbang, S. M. (2022). Quantifying effects of inhomogeneities and curvature on gravitational wave standard siren measurements of H(z). *Phys. Rev. D.* 106, 063514. doi:10.1103/PhysRevD.106.063514

Kolb, E. W., Matarrese, S., Notari, A., and Riotto, A. (2005). Effect of inhomogeneities on the expansion rate of the universe. *Phys. Rev. D.* 71, 023524. doi:10.1103/PhysRevD.71.023524

Krishnan, C., Colgáin, E. Ó., Ruchika, S. A. A., Sheikh-Jabbari, M. M., and Yang, T. (2020). Is there an early universe solution to Hubble tension? *Phys. Rev. D.* 102, 103525. doi:10.1103/PhysRevD.102.103525

Krishnan, C., Ó Colgáin, E., Sheikh-Jabbari, M. M., and Yang, T. (2021). Running Hubble tension and a H0 diagnostic. *Phys. Rev. D.* 103, 103509. doi:10.1103/PhysRevD.103.103509

Kumar, N., and Flanagan, É. É. (2008). Backreaction of superhorizon perturbations in scalar field cosmologies. *Phys. Rev. D.* 78, 063537. doi:10.1103/PhysRevD.78.063537

Kwan, J., Francis, M. J., and Lewis, G. F. (2009). Fractal bubble cosmology: a concordant cosmological model? *MNRAS* 399, L6–L10. doi:10.1111/j.1745-3933.2009.00703.x

Lemaître, G. (1933). L'univers en expansion. *Ann. la Société Sci. Brux.* 53, 51.

Lemaître, G. A., and MacCallum, M. A. H. (1997). The expanding universe. *General Relativ. Gravit.* 29, 641–680. doi:10.1023/A:1018855621348

Lesgourgues, J. (2011). The cosmic linear anisotropy solving system (CLASS) I: overview. *arXiv E-Prints, arXiv:1104.2932*. doi:10.48550/arXiv.1104.2934

Li, N., and Schwarz, D. J. (2007). Onset of cosmological backreaction. *Phys. Rev. D.* 76, 083011. doi:10.1103/PhysRevD.76.083011

Linder, E. V. (2003). Exploring the expansion history of the universe. *Phys. Rev. Lett.* 90, 091301. doi:10.1103/PhysRevLett.90.091301

Maciel, A., Le Delliou, M., and Mimoso, J. P. (2018). Revisiting the Birkhoff theorem from a dual null point of view. *Phys. Rev. D.* 98, 024016. doi:10.1103/PhysRevD.98.024016

MacTavish, C. J., Ade, P. A. R., Bock, J. J., Bond, J. R., Borrill, J., Boscaleri, A., et al. (2006). Cosmological parameters from the 2003 flight of BOOMERANG. *ApJ* 647, 799–812. doi:10.1086/505558

Martineau, P., and Brandenberger, R. (2005). Back-reaction: a cosmological panacea. *arXiv E-Prints, Astro-Ph/0510523*. doi:10.48550/arXiv.astro-ph/0510523

Notari, A. (2006). Late time failure of Friedmann equation. *Mod. Phys. Lett. A* 21, 2997–3007. doi:10.1142/S0217732306021852

Ó Colgáin, E., Sheikh-Jabbari, M. M., and Yin, L. (2021). Can dark energy be dynamical? *Phys. Rev. D.* 104, 023510. doi:10.1103/PhysRevD.104.023510

Okabe, A., Boots, B., and Sugihara, K. (2000). *Spatial tessellations. Concepts and applications of Voronoi diagrams*. John Wiley.

Paranjape, A. (2009). *The averaging problem in cosmology*. Mumbai, India: Tata Institute of Fundamental Research. Ph.D. thesis.

Parry, M. (2006). A rule of thumb for cosmological backreaction. *J. Cosmol. Astropart. Phys.* 2006, 016. doi:10.1088/1475-7516/2006/06/016

Peacock, J. A. (1999). *Cosmological physics*. Cambridge University Press. doi:10.1017/CBO9780511804533

Perlmutter, S. (2003). Supernovae, dark energy, and the accelerating universe. *Phys. Today* 56, 53–62. doi:10.1063/1.1580050

Perlmutter, S., Aldering, G., Goldhaber, G., Knop, R. A., Nugent, P., Castro, P. G., et al. (1999). Measurements of Ω and Λ from 42 high-redshift supernovae. *ApJ* 517, 565–586. doi:10.1086/307221

Planck-Collaboration (2020a). Planck 2018 results. I. Overview and the cosmological legacy of Planck. *A&A* 641, A1. doi:10.1051/0004-6361/201833880

Planck-Collaboration (2020b). Planck 2018 results. VI. Cosmological parameters. *A&A* 641, A6. doi:10.1051/0004-6361/201833910

Poulin, V., Smith, T. L., and Karwal, T. (2023). The ups and downs of early dark energy solutions to the Hubble tension: a review of models, hints and constraints circa 2023. *Phys. Dark Universe* 42, 101348. doi:10.1016/j.dark.2023.101348

Rácz, G., Dobos, L., Beck, R., Szapudi, I., and Csabai, I. (2017). Concordance cosmology without dark energy. *MNRAS* 469, L1–L5. doi:10.1093/mnrasl/slx026

Räsänen, S. (2006a). Accelerated expansion from structure formation. *J. Cosmol. Astropart. Phys.* 2006, 003. doi:10.1088/1475-7516/2006/11/003

Räsänen, S. (2006b). Constraints on backreaction in dust universes. *Class. Quantum Gravity* 23, 1823–1835. doi:10.1088/0264-9381/23/6/001

Rebouças, J., Gordon, J., de Souza, D. H. F., Zhong, K., Miranda, V., Rosenfeld, R., et al. (2024). Early dark energy constraints with late-time expansion marginalization. *J. Cosmol. Astropart. Phys.* 2024, 042. doi:10.1088/1475-7516/2024/02/042

Ricciardelli, E., Quilis, V., and Planelles, S. (2013). The structure of cosmic voids in a ΛCDM universe. *MNRAS* 434, 1192–1204. doi:10.1093/mnras/stt1069

Riess, A. G., Filippenko, A. V., Challis, P., Clocchiatti, A., Diercks, A., Garnavich, P. M., et al. (1998). Observational evidence from supernovae for an accelerating universe and a cosmological constant. *AJ* 116, 1009–1038. doi:10.1086/300499

Riess, A. G., Yuan, W., Macri, L. M., Scolnic, D., Brout, D., Casertano, S., et al. (2022). A comprehensive measurement of the local value of the Hubble constant with 1 km s^{-1} Mpc^{-1} uncertainty from the Hubble space telescope and the SH0ES team. *ApJ* 934, L7. doi:10.3847/2041-8213/ac5c5b

Robertson, H. P. (1935). Kinematics and world-structure. *ApJ* 82, 284. doi:10.1086/143681

Robertson, H. P. (1936a). Kinematics and world-structure ii. *ApJ* 83, 187. doi:10.1086/143716

Robertson, H. P. (1936b). Kinematics and world-structure iii. *ApJ* 83, 257. doi:10.1086/143726

Robertson, B. E., Tacchella, S., Johnson, B. D., Hainline, K., Whitler, L., Eisenstein, D. J., et al. (2023). Identification and properties of intense star-forming galaxies at redshifts z > 10. *Nat. Astron.* 7, 611–621. doi:10.1038/s41550-023-01921-1

Schmidt, B. P., Suntzeff, N. B., Phillips, M. M., Schommer, R. A., Clocchiatti, A., Kirshner, R. P., et al. (1998). The High-Z supernova search: measuring cosmic deceleration and global curvature of the universe using type Ia supernovae. *ApJ* 507, 46–63. doi:10.1086/306308

Scrimgeour, M. I., Davis, T., Blake, C., James, J. B., Poole, G. B., Staveley-Smith, L., et al. (2012). The WiggleZ dark energy survey: the transition to large-scale cosmic homogeneity. *MNRAS* 425, 116–134. doi:10.1111/j.1365-2966.2012.21402.x

Shandarin, S., Feldman, H. A., Heitmann, K., and Habib, S. (2006). Shapes and sizes of voids in the lambda cold dark matter universe: excursion set approach. *MNRAS* 367, 1629–1640. doi:10.1111/j.1365-2966.2006.10062.x

Siegel, E. R., and Fry, J. N. (2005). The effects of inhomogeneities on cosmic expansion. *ApJ* 628, L1–L4. doi:10.1086/432538

Smoot, G. F., Bennett, C. L., Kogut, A., Wright, E. L., Aymon, J., Boggess, N. W., et al. (1992). Structure in the COBE differential microwave radiometer first-year maps. *ApJ* 396, L1. doi:10.1086/186504

Springel, V., White, S. D. M., Jenkins, A., Frenk, C. S., Yoshida, N., Gao, L., et al. (2005). Simulations of the formation, evolution and clustering of galaxies and quasars. *Nature* 435, 629–636. doi:10.1038/nature03597

Steigman, G. (2007). Primordial nucleosynthesis in the precision cosmology era. *Annu. Rev. Nucl. Part. Sci.* 57, 463–491. doi:10.1146/annurev.nucl.56.080805.140437

Stoeger, W. R., Helmi, A., and Torres, D. F. (2007). Averaging Einstein's equations: the linearized case. *Int. J. Mod. Phys. D* 16, 1001–1026. doi:10.1142/S0218271807010535

Tolman, R. C. (1934). Effect of inhomogeneity on cosmological models. *Proc. Natl. Acad. Sci.* 20, 169–176. doi:10.1073/pnas.20.3.169

Tristram, M., Banday, A. J., Douspis, M., Garrido, X., Górski, K. M., Henrot-Versillé, S., et al. (2024). Cosmological parameters derived from the final Planck data release (PR4). *A&A* 682, A37. doi:10.1051/0004-6361/202348015

Tully, R. B., Courtois, H., Hoffman, Y., and Pomarède, D. (2014). The Laniakea supercluster of galaxies. *Nature* 513, 71–73. doi:10.1038/nature13674

Van Acoleyen, K. (2008). Lemaitre-Tolman-Bondi solutions in the Newtonian gauge: from strong to weak fields. *J. Cosmol. Astropart. Phys.* 2008, 028. doi:10.1088/1475-7516/2008/10/028

van de Weygaert, R. (1994). Fragmenting the Universe. 3: the constructions and statistics of 3-D Voronoi tessellations. *A&A* 283, 361–406.

van de Weygaert, R., and Icke, V. (1989). Fragmenting the universe. II - Voronoi vertices as abell clusters. *A&A* 213, 1–9.

von Hausegger, S. (2024). The expected kinematic matter dipole is robust against source evolution. *MNRAS* 535, L49–L53. doi:10.1093/mnrasl/slae092

Voronoi, G. (1908). Nouvelles applications des paramétres continus á la théorie des formes quadratiques. deuxiéme mémoire. recherches sur les parallélloédres primitifs. *J. für die reine und angewandte Math.* 134, 198–287.

Walker, A. G. (1937). On Milne's theory of world-structure. *Proc. Lond. Math. Soc.* 42, 90–127. doi:10.1112/plms/s2-42.1.90

Weinberg, S. (2008). *Cosmology*. Oxford, UK: Oxford University Press.

Wetterich, C. (2003). Can structure formation influence the cosmological evolution? *Phys. Rev. D.* 67, 043513. doi:10.1103/PhysRevD.67.043513

Wiltshire, D. L. (2007). Cosmic clocks, cosmic variance and cosmic averages. *New J. Phys.* 9, 377. doi:10.1088/1367-2630/9/10/377

Wiltshire, D. L. (2011). What is dust? Physical foundations of the averaging problem in cosmology. *Class. Quantum Gravity* 28, 164006. doi:10.1088/0264-9381/28/16/164006